

The *Arabidopsis* Chaperone J3 Regulates the Plasma Membrane H⁺-ATPase through Interaction with the PKS5 Kinase

Yongqing Yang,^{a,b,c,1} Yunxia Qin,^{d,1} Changgen Xie,^{a,b,1} Feiyi Zhao,^{e,1} Jinfeng Zhao,^b Dafa Liu,^d Shouyi Chen,^e Anja T. Fuglsang,^f Michael G. Palmgren,^f Karen S. Schumaker,^g Xing Wang Deng,^a and Yan Guo^{b,c,2}

^a College of Life Sciences, Peking University, Beijing 100871, China

^b National Institute of Biological Sciences, Beijing 102206, China

^c State Key Laboratory of Plant Physiology and Biochemistry, College of Biological Sciences, China Agricultural University, Beijing 100094, China

^d Key Lab of Ministry of Agriculture for Biology of Rubber Tree, Rubber Research Institute, Chinese Academy of Tropical Agricultural Sciences, Danzhou, Hainan 571737, China

^e Institute of Genetics and Developmental Biology, Chinese Academy of Sciences, Beijing, 100101 China

^f Department of Plant Biology, University of Copenhagen, DK-1871 Frederiksberg C, Denmark

^g Department of Plant Sciences, University of Arizona, Tucson, Arizona 85721

The plasma membrane H⁺-ATPase (PM H⁺-ATPase) plays an important role in the regulation of ion and metabolite transport and is involved in physiological processes that include cell growth, intracellular pH, and stomatal regulation. PM H⁺-ATPase activity is controlled by many factors, including hormones, calcium, light, and environmental stresses like increased soil salinity. We have previously shown that the *Arabidopsis thaliana* Salt Overly Sensitive2-Like Protein Kinase5 (PKS5) negatively regulates the PM H⁺-ATPase. Here, we report that a chaperone, J3 (DnaJ homolog 3; heat shock protein 40-like), activates PM H⁺-ATPase activity by physically interacting with and repressing PKS5 kinase activity. Plants lacking J3 are hypersensitive to salt at high external pH and exhibit decreased PM H⁺-ATPase activity. J3 functions upstream of PKS5 as double mutants generated using *j3-1* and several *pks5* mutant alleles with altered kinase activity have levels of PM H⁺-ATPase activity and responses to salt at alkaline pH similar to their corresponding *pks5* mutant. Taken together, our results demonstrate that regulation of PM H⁺-ATPase activity by J3 takes place via inactivation of the PKS5 kinase.

INTRODUCTION

In both plants and fungi, transport across the plasma membrane (PM) is energized by an electrochemical gradient of protons (H⁺). These gradients are established by the electrogenic PM H⁺ pumps (ATPases), which convert chemical energy derived from hydrolysis of ATP into pH and electrical gradients across the plasma membrane (Palmgren, 2001). The combined electrochemical gradient constitutes a driving force for the transport of solutes and metabolites across the plasma membrane (Morsomme and Boutry, 2000).

In *Arabidopsis thaliana*, PM H⁺-ATPases are encoded by a 12-member gene family (*AHA1* to *AHA12*; Palmgren, 2001). These H⁺-ATPases play regulatory roles in signal transduction, during cell expansion, turgor regulation, in the regulation of intracellular pH, and in the response of the plant to increases in soil salinity

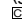
(Palmgren, 2001; Rober-Kleber et al., 2003; Fuglsang et al., 2007; Gevaudant et al., 2007; Merlot et al., 2007). A number of factors, including hormones (auxin and abscisic acid [ABA]), calcium, blue light, and fungal elicitors, have been shown to elicit changes in cellular pH through regulation of the PM H⁺-ATPase (Kinoshita et al., 1995; Xing et al., 1997; Kim et al., 2001; Brault et al., 2004; Zhang et al., 2004). For example, auxin activates the H⁺-ATPase, resulting in apoplastic acidification, a process leading to cell wall loosening and cell and organ elongation (Rober-Kleber et al., 2003). Exogenous application of ABA on leaves has an inhibitory effect on PM H⁺-ATPase activity (Roelfsema et al., 1998; Zhang et al., 2004), while mutations in the PM H⁺-ATPase *AHA1* (*ost2*) result in a constitutively active protein and plants with reduced sensitivity to ABA during stomatal movement (Merlot et al., 2007). Evidence also exists linking PM H⁺-ATPase activity and increased salt tolerance as overexpression of an activated PM H⁺-ATPase increased plant salt tolerance (Gevaudant et al., 2007). This regulation appears to be due to posttranslational modification of the protein based on the fact that PM H⁺-ATPase protein levels do not change when plants are grown in salt (Ayala et al., 1996; Wu and Seliskar, 1998; Morsomme and Boutry, 2000).

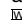
One well-characterized mechanism underlying regulation of PM H⁺-ATPase activity involves an autoinhibitory domain in

¹ These authors contributed equally to this work.

² Address correspondence to guoyan@cau.edu.cn.

The author responsible for distribution of materials integral to the findings presented in this article in accordance with the policy described in the Instructions for Authors (www.plantcell.org) is: Yan Guo (guoyan@cau.edu.cn).

 Some figures in this article are displayed in color online but in black and white in the print edition.

 Online version contains Web-only data.

www.plantcell.org/cgi/doi/10.1105/tpc.109.069609

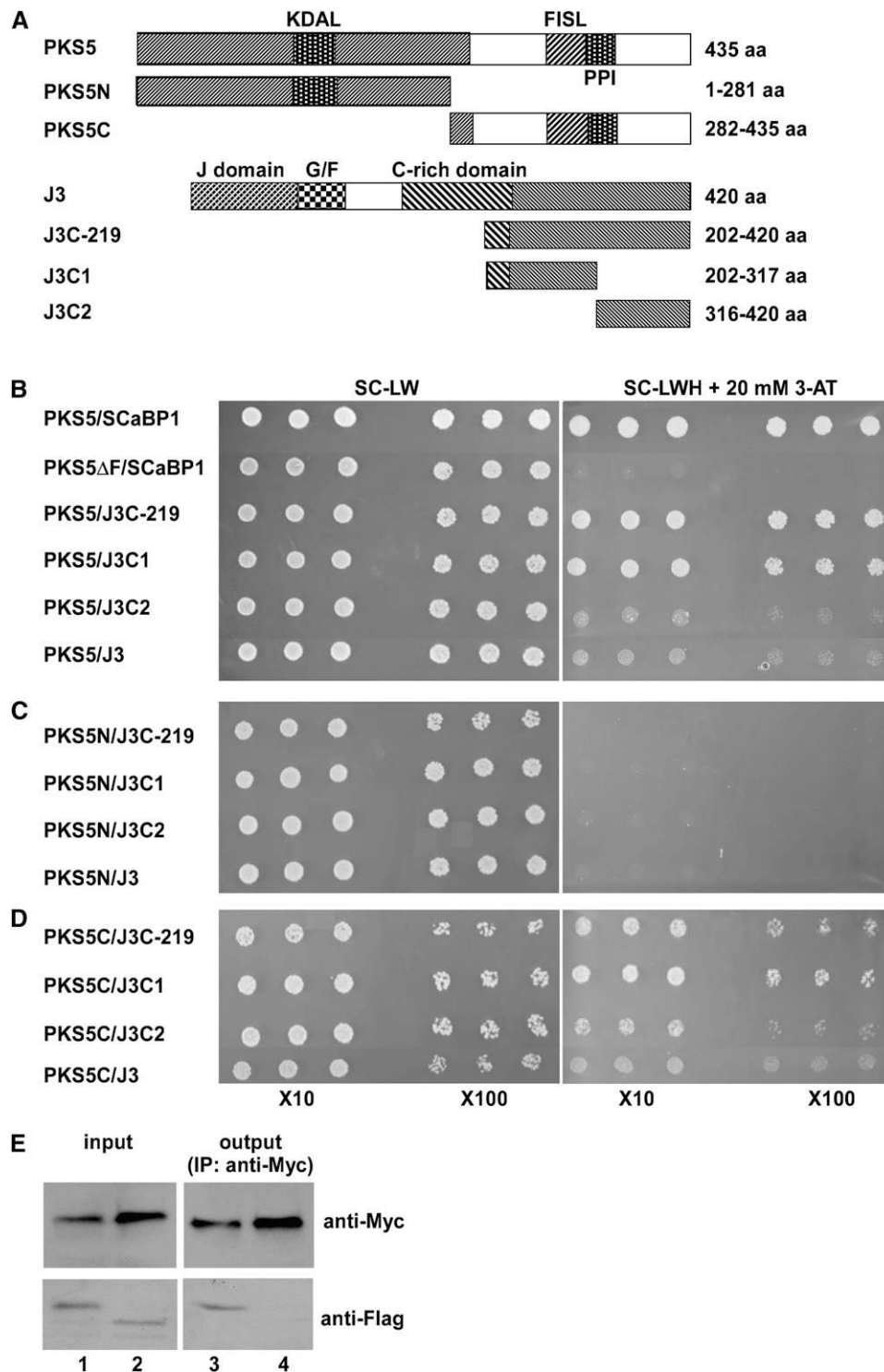


Figure 1. PKS5 Interacts with J3.

(A) Schematic diagram of the PKS5, PKS5N, PKS5C, J3, J3C-219, J3C1, and J3C2 proteins used in the yeast two-hybrid analysis. KDAL, kinase activation loop; FISL, SCaBP interaction domain; PPI, phosphatase interaction domain; J-domain, DnaJ domain; G/F, domain rich in Gly and Phe residues; C-rich domain, a distal zinc finger (CxxCxGxG)₄ domain.

(B) to (D) Yeast two-hybrid analysis of interactions between the full-length PKS5 protein (PKS5) or the N- (PKS5N) or C- (PKS5C) terminal portions of the protein with J3, or J3C-219, J3C1, or J3C2. Interactions between the full-length PKS5 protein or the protein with the FISL domain deleted (PKS5 Δ F) and

C-terminal region of the protein (Palmgren et al., 1991). Phosphorylation of this C-terminal autoinhibitory domain at the penultimate residue (Thr-947) leads to its interaction with a 14-3-3 regulatory protein and activation of the H⁺-ATPase (Svennelid et al., 1999; Camoni et al., 2000; Gevaudant et al., 2007). The activated protein complex is likely to consist of six phosphorylated PM H⁺-ATPase molecules assembled in a hexameric structure together with six 14-3-3 molecules (Kanczewska et al., 2005; Ottmann et al., 2007). We recently demonstrated that the PKS5 protein kinase negatively regulates the activity of the PM H⁺-ATPase by directly phosphorylating the AHA2 isoform of the enzyme in its C-terminal regulatory domain at Ser-931 and that this phosphorylation inhibits the interaction between AHA2 and the 14-3-3 protein (Fuglsang et al., 2007). A role for PKS5 in the regulation of the PM H⁺-ATPase was further supported by the recent demonstration that Ser-938 (identical to Ser-931 in AHA2 in *Arabidopsis*) is phosphorylated in vivo in PMA2, a PM-H⁺-ATPase isoform in tobacco (*Nicotiana tabacum*; Duby et al., 2009).

Environmental stresses in plants often cause protein denaturation; therefore, maintaining proteins in their functional conformations and preventing protein aggregation are particularly important for cell survival under stress conditions. Molecular chaperones (heat shock proteins [Hsps]) are key components contributing to cellular homeostasis under adverse growth conditions (Wang et al., 2004). DnaJ/Hsp40 was originally characterized in *Escherichia coli* as a 41-kD heat shock protein that interacts directly with DnaK and GrpE constituting a molecular chaperone machine (Georgopoulos et al., 1980; Liberek et al., 1991; Scidmore et al., 1993; Bukau and Horwich, 1998; Goffin and Georgopoulos, 1998; Miernyk, 1999). Additionally, DnaJ can act independently as a chaperone (Laufen et al., 1999). Most DnaJ proteins contain a J-domain, a proximal G/F-domain, and a distal zinc finger (CxxCxGxG)₄ domain, followed by less conserved C-terminal sequences (Caplan et al., 1993; Silver and Way, 1993). The J domain, a 70-amino acid sequence, contains four helices and a highly conserved tripeptide made up of His, Pro, and Asp (the HPD motif) in the loop region between helices II and III (Qian et al., 1996). The J domain binds to Hsp70s, and this binding stabilizes Hsp70 interaction with substrate proteins (Qiu et al., 2006). The G/F-domain, which is rich in Gly and Phe residues and comprises a flexible linker region, helps to confer interaction specificity among DnaK, DnaJ, and target polypeptides (Wall et al., 1995; Yan and Yan, 1999). The distal zinc finger domain is believed to participate in protein-protein interactions among DnaJ, DnaK, and target polypeptides (Banecki et al., 1996; Szabo et al., 1996). DnaJ has been conserved throughout

evolution and is important for protein translation, folding, unfolding, translocation, and degradation in a broad array of cellular processes (Boston et al., 1996; Waters et al., 1996; Wang et al., 2004). Expression of Hsps in planta is induced by high temperature and also by a wide range of other environmental stresses, including increased soil salinity and osmotic, water, cold, and oxidative stresses (Boston et al., 1996; Waters et al., 1996; Wang et al., 2004). In addition to their function as chaperon proteins, DnaJs are also involved in other biological processes, including regulation of transcriptional activation by directly binding transcription factors (Ham et al., 2006), formation of endosomes (Tamura et al., 2007), and in carotenoid accumulation (Lu et al., 2006). There are 89 putative J-domain proteins predicted in *Arabidopsis* (Miernyk, 2001). These J-domain proteins are both soluble and found in membrane compartments of all cellular organelles (Miernyk, 2001). J3 (*Arabidopsis* DnaJ homologous protein3) contains all typical functional domains found in J-domain family members (Zhou and Miernyk, 1999). J3 is expressed in roots, stems, leaves, flower buds, flowers, and siliques, and its expression can be induced by heat and water stress (Zhou and Miernyk, 1999; Li et al., 2005).

In this study, we identify a DnaJ-like protein, *Arabidopsis* J3, as a positive regulator of the PM H⁺-ATPase. We show that J3 interacts with and represses activity of the PKS5 kinase. Together with results from our genetic studies, we demonstrate that J3 regulates PM H⁺-ATPase activity through interaction with the PKS5 kinase.

RESULTS

PKS5 Interacts with J3

To understand how PKS5 regulates the PM H⁺-ATPase, we identified PKS5-interacting proteins using yeast two-hybrid assays. To do this, we cloned the *PKS5* cDNA into the pAS2 vector and transformed the resulting plasmid into yeast strain Y190. PKS5 was then used as bait to screen an *Arabidopsis* cDNA library (obtained from The Arabidopsis Information Resource [TAIR]). Two positive clones were sequenced and found to include 219 amino acids (J3C-219) that are identical to the C terminus of At3g44110, which encodes a putative cochaperone DnaJ-like heat shock protein (J3) (Zhou and Miernyk, 1999). To narrow down the interaction domain in J3, J3C-219 was divided into two parts, J3C1 (amino acids 202 to 317) and J3C2 (amino acids 316 to 420); the structures of the peptides are shown in Figure 1A. These fragments and the full-length J3 were cloned

Figure 1. (continued).

SCaBP1 were used as positive and negative controls, respectively. Yeast lines harboring the indicated plasmids were grown on synthetic complete (SC) medium without Leu and Trp (SC-LW, left panel) and on SC medium without Leu, Trp, and His (SC-LWH) and with 20 mM 3-amino-1,2,4-triazole (3-AT; right panel). Yeast cells were incubated until OD₆₀₀ = 1 and then diluted 10- or 100-fold and used for assays.

(E) Coimmunoprecipitation of PKS5 and J3 proteins in vivo. The 35SP:6×Myc-J3 plasmid was cotransformed into wild-type (Col-0) protoplasts with 35SP:3×FLAG-PKS5 (lanes 1 and 3) or 35SP:3×FLAG-TTG1 (lanes 2 and 4). Total protein extracts were analyzed with immunoblots using anti-Myc and anti-FLAG antibodies to detect the presence of PKS5, J3, or TTG1 (input). Immunoprecipitation was performed using anti-Myc agarose conjugate, and the products were analyzed with immunoblots using anti-FLAG antibody to detect coimmunoprecipitated FLAG-PKS5 (lane 3) or FLAG-TTG1 (lane 4).

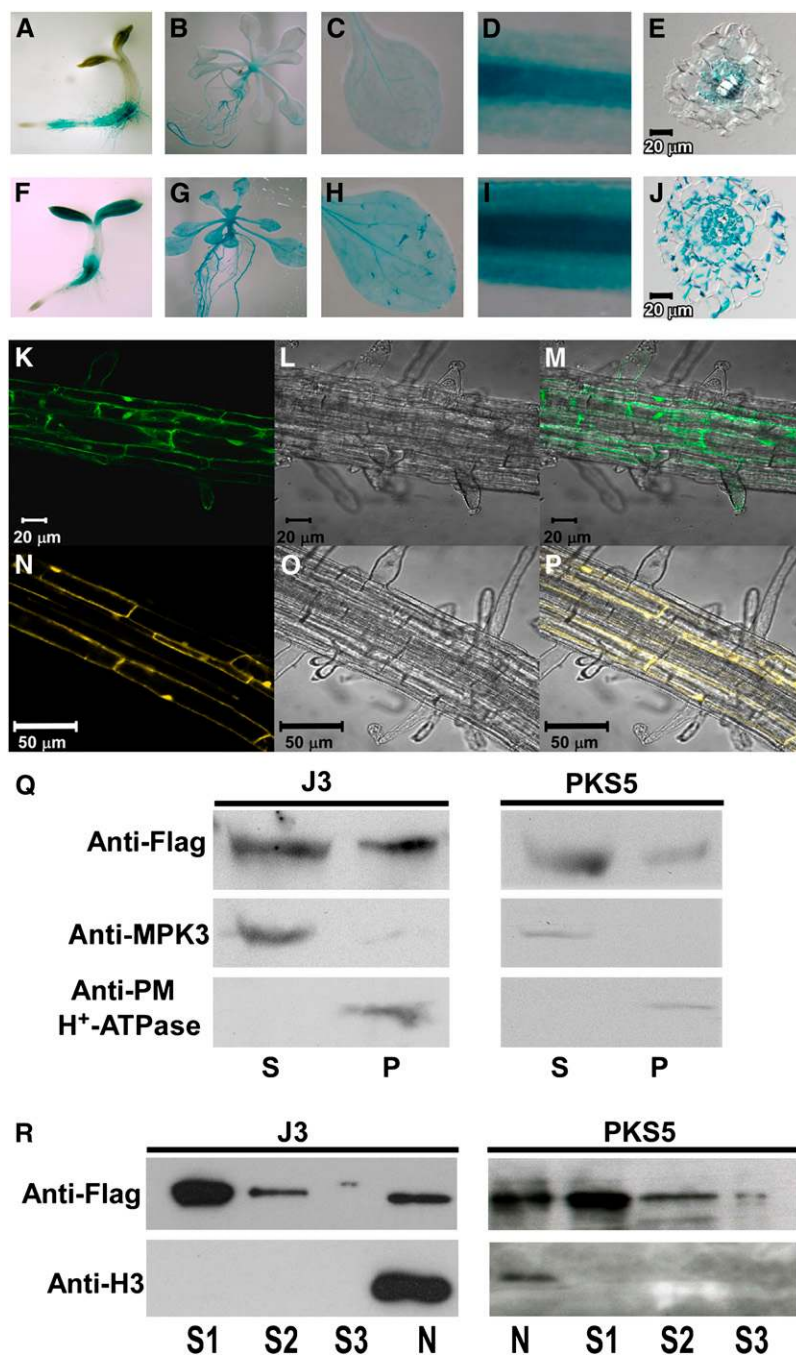


Figure 2. PKS5 and J3 Have Overlapping Tissue-Specific Expression and Subcellular Localization.

(A) to (J) Expression of *J3* and *PKS5* in 3-d-old seedlings [(A) and (F)], 10-d-old seedlings [(B) and (G)], rosette leaves [(C) and (H)], roots [(D) and (I)], and cross sections of roots [(E) and (J)].

(A) to (E) *PKS5* promoter-*GUS* expression in wild-type seedlings.

(F) to (J) *J3* promoter-*GUS* expression in wild-type seedlings.

(K) to (P) Subcellular localization of GFP-*J3* [(K) to (M)] and *PKS5*-YFP [(N) to (P)] in the upper portion of the root. Confocal GFP images [(K) and (N)], bright-field images [(L) and (O)], and combined GFP and bright-field images [(M) and (P)].

(Q) Both of *PKS5* and *J3* were detected in soluble and plasma membrane-enriched fractions. Isolation of plasma membrane vesicles was by two-phase partitioning from seedlings of *j3-1* plants expressing *35SP::3×flag-J3* or *pks5-1* plants expressing *DexP::3×flag-PKS5*. Equal amount of soluble (S) and plasma membrane (P) proteins were separated by SDS-PAGE followed by analysis with anti-flag, anti-MAPK3, or anti-PM H⁺-ATPase antibodies.

(R) Both of *PKS5* and *J3* were detected in nucleus. Nuclei were isolated from seedlings of *j3-1* plants expressing *35SP::3×flag-J3* or *pks5-1* plants expressing *DexP::3×flag-PKS5*. The nuclei pellet was then washed three times. Equal amount of three washing (S1-S3) and nuclei (N) proteins were separated by SDS-PAGE followed by analysis with anti-flag or anti-Histone H3 antibodies.

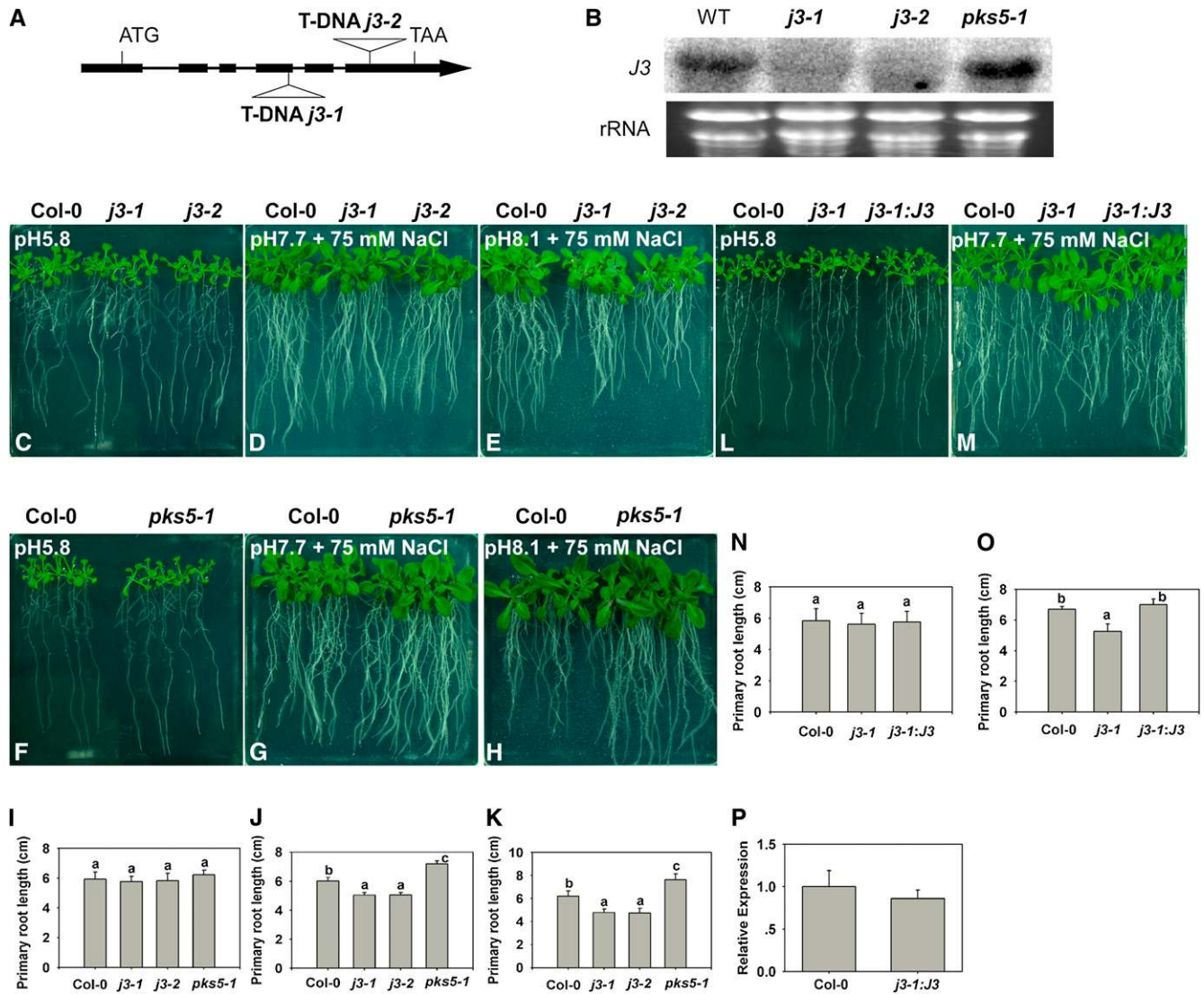


Figure 3. *j3* Mutants Have Increased Sensitivity to Salt in Alkaline Conditions.

(A) Schematic diagram of the *J3* gene showing the T-DNA insertion sites in the *j3-1* and *j3-2* mutants. The filled black boxes represent exons, while the lines between the boxes represent introns. The two T-DNA insertions are also indicated.

(B) Transcript levels of *J3* are undetectable in the *j3-1* and *j3-2* mutants. Total RNA was isolated from 10-d-old seedlings of Col-0, *j3-1*, *j3-2*, and *pks5-1* mutants. RNA (15 μg) from each sample was used for RNA gel blot analysis. Ethidium bromide staining of rRNA is included as a loading control.

(C) to (O) Five-day-old Col-0, *pks5-1*, *j3-1*, *j3-2*, and *j3-1* expressing 35SP: *J3* seedlings grown on MS medium at pH 5.8 were transferred to MS medium at pH 5.8, at pH 7.7 with 75 mM NaCl, or at pH 8.1 with 75 mM NaCl. Photographs in **(C)**, **(F)**, and **(L)** were taken 7 d after transfer; in **(D)**, **(G)**, and **(M)**, 14 d after transfer; in **(E)** and **(H)**, 21 d after transfer.

(I) and **(N)** Primary root elongation of plants transferred to MS medium at pH 5.8.

(J) and **(O)** Primary root elongation of plants transferred to MS medium at pH 7.7 with 75 mM NaCl.

(K) Primary root elongation of plants transferred to MS medium at pH 8.1 with 75 mM NaCl.

(P) Relative expression of *j3-1* expressing 35SP: *J3* with *J3* real-time quantitative RT-PCR.

In **(I)** and **(N)**, primary root length was measured 7 d after transfer; **(J)** and **(O)**, primary root length was measured 14 d after transfer; **(K)**, primary root length was measured 21 d after transfer. Error bars represent SD (plant number >15). A Student's *t* test was used to determine statistical significance; significant differences ($P \leq 0.05$) in **(I)** to **(K)**, **(N)**, and **(O)** are indicated by different lowercase letters.

[See online article for color version of this figure.]

into the pACT2 vector, and combinations of PKS5 and J3 were cotransformed into yeast. Both the J3C1 and J3C2 peptides interacted with the full-length PKS5 protein and the C terminus of PKS5, with J3C1 showing a stronger interaction than J3C2 (Figure 1B). The PKS5 protein interacted weakly with J3 (Figure 1B). To determine the region of PKS5 that interacts with J3, fragments encoding the N-terminal kinase domain (PKS5N, amino acids 1 to 281) or the C-terminal regulatory domain (PKS5C, amino acids 282 to 435) of PKS5 were cloned into pAS2, and these two plasmids were cotransformed with the J3 plasmids into yeast. The PKS5 kinase domain (N terminus) did not interact with any portion of J3 (Figure 1C). The PKS5 C terminus interacted with J3C1, which showed a stronger interaction than any other J3 fragment (Figure 1D). As controls, PKS5 was shown to interact with SOS3-LIKE CALCIUM BINDING PROTEIN1 (SCaBP1), and this interaction was abolished when the FISL domain (a domain in the PKS5 protein required for SCaBP binding) was deleted (PKS5 Δ F, Figure 1B).

To determine if this interaction exists *in vivo*, three FLAG tags in a tandem repeat were fused to *PKS5* or to the trichome-associated gene *TRANSPARENT TESTA GLABRA1* (*TTG1*) at their N termini, and six Myc tags in a tandem repeat were fused to *J3* at its N terminus with fusions for all three genes under the control of the 35S promoter. Combinations of 6 \times Myc-*J3* and 3 \times FLAG-*TTG1* or 6 \times Myc-*J3* and 3 \times FLAG-*PKS5* were cotransfected into *Arabidopsis* leaf protoplasts. The 6 \times Myc-*J3* protein was immunoprecipitated using anti-Myc conjugated agarose. After washing, immunoblots were probed with anti-FLAG antibody. The 3 \times FLAG-*PKS5* but not 3 \times FLAG-*TTG1* protein was pulled down by 6 \times Myc-*J3* (Figure 1E), suggesting that *PKS5* and *J3* can function in the same complex. Together with the yeast two-hybrid results, our data indicate that *PKS5* and *J3* interact *in vivo*.

PKS5 and J3 Have Overlapping Tissue-Specific Expression and Subcellular Localization

To determine if *PKS5* and *J3* colocalize in planta, we monitored *PKS5* and *J3* tissue specific expression using two approaches. First, a 1918-bp DNA fragment upstream of the *J3* translational start codon was amplified and cloned into pCambia1301 transcriptionally fused to β -glucuronidase (*GUS*) and the resulting plasmid was transformed into Columbia-0 (Col-0). *GUS* signals driven by the *PKS5* (Fuglsang et al., 2007) or *J3* promoter are shown in Figures 2A to 2E and 2F to 2J, respectively. Both J3P: *GUS* and PKS5P: *GUS* were expressed in the roots and leaves of seedlings with stronger *GUS* staining in vascular tissue (Figure 2). In cross sections of the root, PKS5P: *GUS* was mainly observed in phloem (Figure 2E), which is consistent with previous findings (Fuglsang et al., 2007), while the J3P: *GUS* signal was observed in epidermal cells, the cortex, phloem, and xylem parenchyma cells (Figure 2J); this expression pattern is similar to that of *AHA2P: GUS* (Fuglsang et al., 2007). We also analyzed the tissue-specific expression of *PKS5* and *J3* using quantitative real-time PCR. Total RNA was extracted from roots, stems, rosette leaves, cauline leaves, flowers, and siliques of 40-d-old Col-0 plants. Both *PKS5* and *J3* were constitutively expressed in all tissues

with highest expression in reproductive and root tissues (see Supplemental Figure 1 online).

To learn more about the interaction between *PKS5* and *J3*, we determined the subcellular localization of the two proteins. The green fluorescent protein (GFP) reporter was fused to both proteins at their N termini under the control of the 35S promoter, and the resulting plasmids were transformed into the *Arabidopsis* Col-0 genetic background. Transgenic plants in the T2 generation were tested for GFP localization using confocal microscopy. GFP-*J3* was detected at the cell membrane, in the cytoplasm, and in the nucleus (Figures 2K to 2M); however, no GFP-*PKS5* signal was detected in >100 35SP:GFP-*PKS5* transgenic lines. We then fused yellow fluorescent protein (YFP) to the C terminus of *PKS5* under the control of a dexamethasone-inducible promoter (Aoyama and Chua, 1997), and the YFP signal was analyzed in transgenic plants treated with 10 mM dexamethasone. As was found for GFP-*J3*, *PKS5* localized to the cell membrane, in the cytoplasm, and in the nucleus (Figures 2N to 2P).

To further analyze the subcellular localization of *PKS5* and *J3* in plant cells, we fused a 3 \times FLAG tag at the N terminus of *PKS5* under the control of a dexamethasone-inducible promoter and 3 \times FLAG tag at the N terminus of *J3* driven by the 35S promoter. The resulting plasmids and 35SP:GFP-*J3* were transferred into their corresponding mutants and the mutant phenotypes were rescued by the transgenes (see Supplemental Figures 2 and 3 online). We then isolated nuclei, a plasma membrane-enriched fraction, and a soluble fraction from the transgenic plants expressing 35SP:3 \times FLAG-*J3* and DexP:3 \times FLAG-*PKS5* and analyzed the immunoblots with anti-FLAG antibody. As shown in Figure 2Q and 2R, the tagged *PKS5* and *J3* proteins were detected in all three fractions. These results are consistent with our *PKS5*-YFP and GFP-*J3* results (Figures 2K to 2P). Using the same protein samples, as expected, MITOGEN-ACTIVATED PROTEIN KINASE3, the PM H⁺-ATPase, and histone H3 were found in the soluble, plasma membrane-enriched and nuclear fractions, respectively. To further determine the purity of the phase partitioned membrane fractions, anti-Arf1 (ADP-ribosylation factor 1, a Golgi apparatus marker) and anti-Sar1 (secretion-associated and Ras-related protein 1, an endoplasmic reticulum marker) antibodies were used to investigate the presence of endoplasmic reticulum and Golgi membranes in the plasma membrane-enriched fraction. Both proteins were at undetectable levels in the plasma membrane-enriched fraction. Consistent with a previous study (Pimpl et al., 2000), these proteins were detected in total membrane and soluble fractions (see Supplemental Figure 4 online). Together, these data demonstrate that the gene expression and protein localization of *J3* and *PKS5* overlap during *Arabidopsis* development.

***j3* Mutants Have Increased Sensitivity to Salt in Alkaline Conditions**

To determine if *J3* and *PKS5* have similar functions, we obtained two *J3* T-DNA insertion lines from TAIR (SALK_132923 and SALK_141625). The positions of the T-DNA insertions are shown in Figure 3A. Homozygous T-DNA lines, *j3-1* and *j3-2*, were identified using T-DNA left border primers and *J3* gene-specific

primers. To determine if expression of *J3* is abolished in these two lines, total RNA was extracted from 10-d-old Col-0, *pk5-1* (a *PKS5* loss-of-function mutant; Fuglsang et al., 2007), and *j3-1* and *j3-2* seedlings and analyzed using RNA gel blots. The expression of *J3* could not be detected in *j3-1* and *j3-2*; however, it is present in Col-0 and *pk5-1* (Figure 3B; see Supplemental Figure 5 online). We have previously shown that *PKS5* is a negative regulator of the PM H⁺-ATPase and that *PKS5* loss-of-function mutants are resistant to high pH in the external medium (Fuglsang et al., 2007). When we monitored *j3* mutant seedling growth in response to alkaline pH, no consistent, significant difference was detected between Col-0 and mutant plants. In nature, soil alkalinity is often associated with increased soil salinity partly due to application of fertilizers and irrigation water (Richards, 1954). Alkaline conditions significantly increased the salt sensitivity of *Arabidopsis* (see Supplemental Figure 6 online). To determine if the *j3* mutants have increased sensitivity to salinity in alkaline conditions, 5-d-old seedlings of Col-0, *j3-1*, and *j3-2* grown on Murashige and Skoog (MS) medium at pH 5.8

were transferred to medium at pH 5.8, pH 7.7 with 75 mM NaCl, or pH 8.1 with 75 mM NaCl. No significant difference in growth was detected between Col-0 and the *j3* mutants on medium at pH 5.8 (Figures 3C and 3I; see Supplemental Figure 7A online). On medium at pH 7.7 with 75 mM NaCl (Figures 3D and 3J; see Supplemental Figure 7B online), root elongation in the *j3* mutants was reduced compared with that of Col-0, and this reduction in growth was even more pronounced at pH 8.1 in the presence of 75 mM NaCl (Figures 3E and 3K; see Supplemental Figure 7C online). By contrast, when we grew Col-0 and *pk5-1* seedlings on the same media, primary root elongation in *pk5-1* seedlings was less sensitive to NaCl in alkaline conditions relative to the growth of wild-type plants (Figures 3G, 3H, 3J, and 3K). This result is consistent with our previous finding that *pk5-1* is more tolerant to alkaline pH than Col-0 (Fuglsang et al., 2007). When we tested the sensitivity of the *j3-1* transgenic plants expressing *35SP:J3* to salinity in alkaline conditions, we found the mutant phenotype was rescued by the transgene (Figures 3L to 3P; see Supplemental Figures 7D and 7E online).

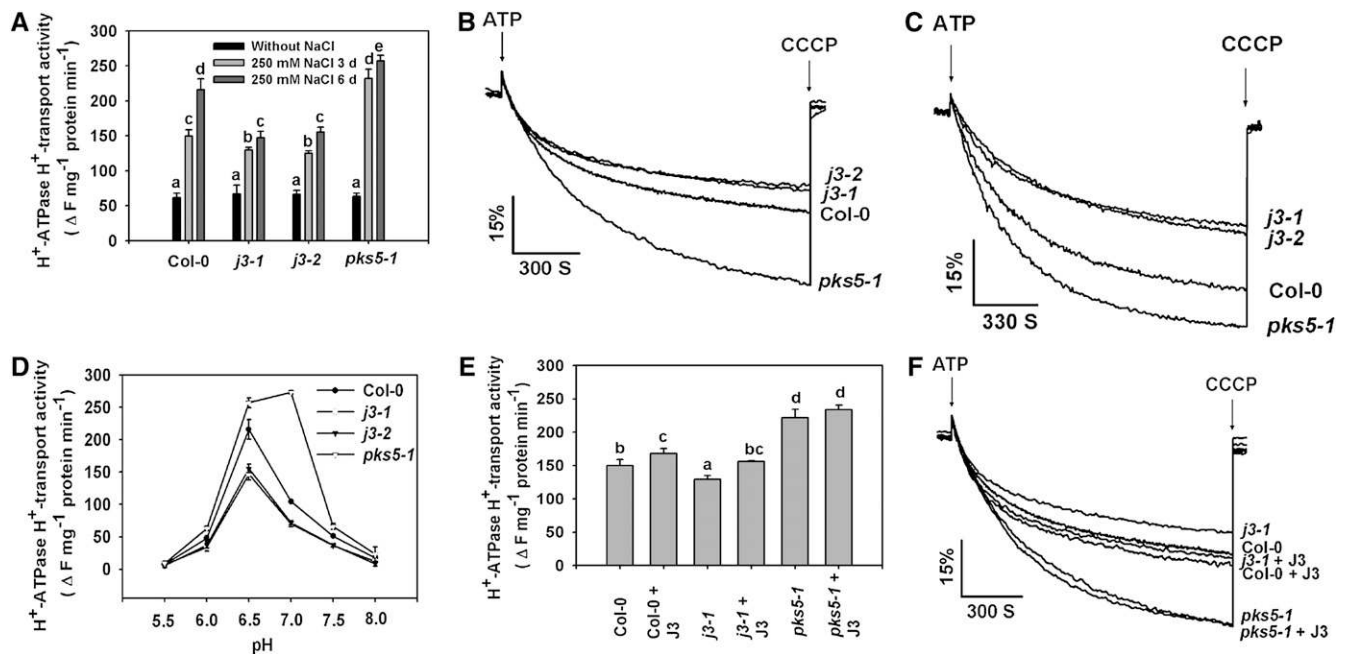


Figure 4. J3 Positively Regulates PM H⁺-ATPase Activity.

Plasma membrane vesicles were isolated from Col-0, *pk5-1*, *j3-1*, and *j3-2* mutant plants treated with or without 250 mM NaCl for 3 or 6 d. PM H⁺-ATPase activity (H⁺-transport resulting in intravesicular acidification and pH gradient [Δ pH] formation) was initiated by addition of 3 mM ATP, and the Δ pH was collapsed by addition of 10 μ M (final concentration) carbonyl cyanide m-chlorophenylhydrazone (CCCP).

(A) Comparison of PM H⁺-ATPase activity in vesicles isolated from Col-0, *j3-1*, *j3-2*, and *pk5-1* plants treated with or without 250 mM NaCl for 3 or 6 d. **(B)** and **(C)** PM H⁺-ATPase activity was measured in the vesicles isolated from Col-0, *j3-1*, *j3-2*, and *pk5-1* plants treated with 250 mM NaCl for 3 d **(B)** or 6 d **(C)**.

(D) PM H⁺-ATPase activity was measured at different pH.

(E) Comparison of PM H⁺-ATPase activity in the presence of 250 ng/mL recombinant J3 protein in vesicles isolated from Col-0, *j3-1*, and *pk5-1* plants.

(F) PM H⁺-ATPase activity was measured in the presence of 250 ng/mL recombinant J3 protein in vesicles isolated from Col-0, *j3-1*, and *pk5-1* plants. Units of PM H⁺-ATPase activity (H⁺-transport) are change in fluorescence (Δ F) per min per mg protein.

All data represent means \pm SE of at least three replicate experiments. Each replicate was performed using independent membrane preparations. One representative experiment of three replicates is shown in **(B)** and **(C)**. A Student's *t* test was used to determine statistical significance; significant differences ($P \leq 0.05$) in **(A)** and **(E)** are indicated by different lowercase letters.

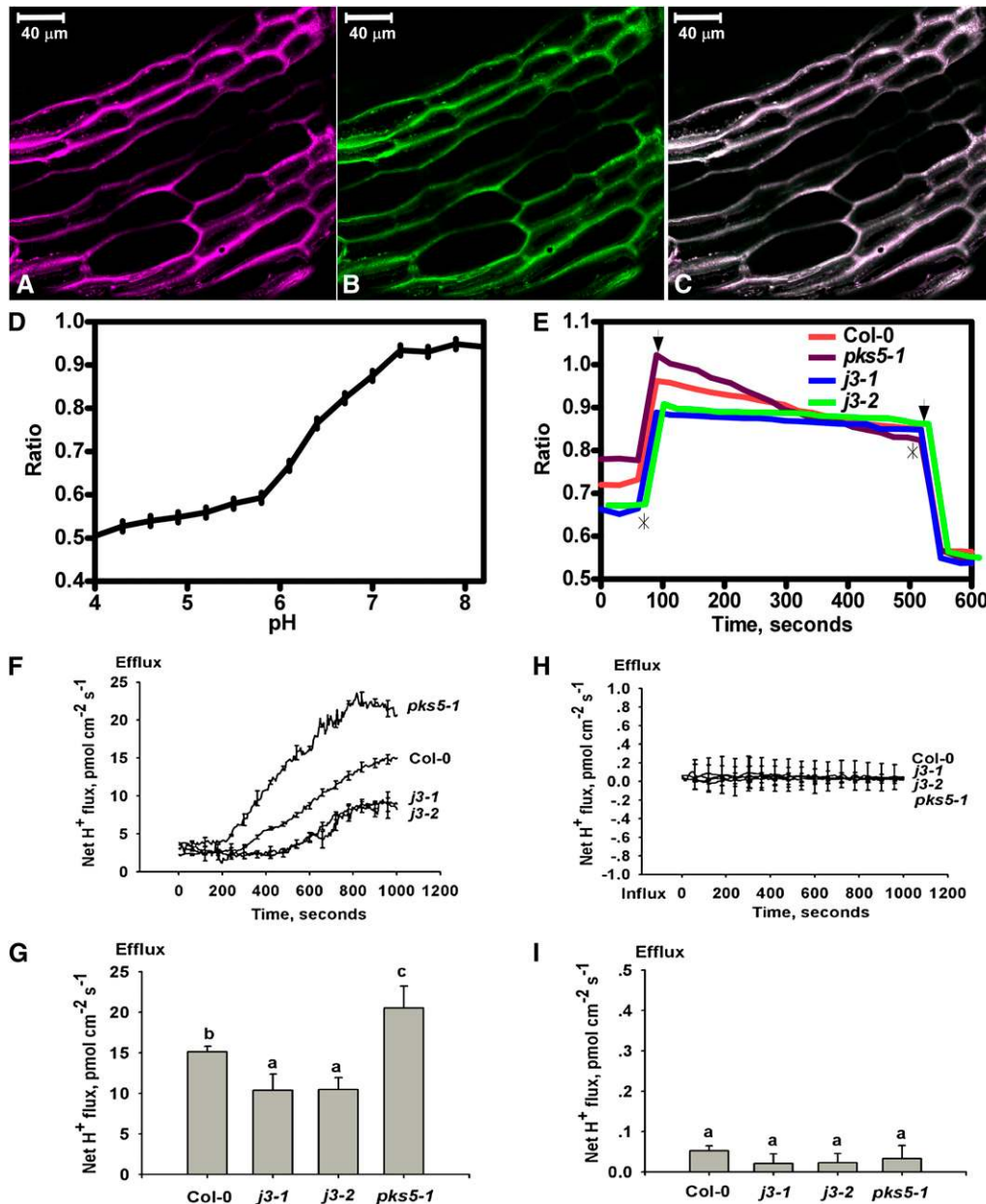


Figure 5. Proton Efflux Decreases in the Root of *j3* Mutant Plants.

The pH sensitive ratiometric probe D-1950, a dextran-conjugated membrane impermeable fluorescence dye, was used to measure proton secretion in the upper region of the root, and MIFE assays were used for proton efflux measurements at the root apex.

(A) to (E) pH ratio imaging in the apoplast of Col-0, *pks5-1*, *j3-1*, and *j3-2* roots.

(A) Fluorescence of fluorescein in pseudocolor.

(B) Fluorescence of rhodamine in pseudocolor.

(C) Overlay of the fluorescein and rhodamine fluorescence in pseudo colors. Bars = 40 μm .

(D) pH calibration curve showing the response of the probe D-1950 at different pH buffers regimes.

(E) Mean value ratio curve for mutant ($n = 20$) and Col-0 ($n = 17$) plants. Ratios were calculated as fluorescein/rhodamin fluorescence levels. The slope in each experiment was calculated and used in one-way analysis of variance. Asterisks show where pH regimes were shifted upwards to pH 8.4 and downwards to pH 5.8, respectively. Arrows indicate the two outer points used to define the area from where the slope was calculated.

(F) to (I) The net proton effluxes in roots of Col-0, *pks5-1*, *j3-1*, and *j3-2* plants. The MIFE technique was used for noninvasive ion flux measurement. (F) Net proton effluxes in Col-0, *pks5-1*, *j3-1*, and *j3-2* root tips. After roots were treated with alkaline conditions (pH 7.7) plus 75 mM NaCl, transient net H^+ fluxes were recorded.

(G) Calculated net proton effluxes from (F).

J3 Positively Regulates PM H⁺-ATPase Activity

Because J3 interacts with PKS5 and loss-of-function *j3* and *pks5-1* mutants have opposite responses to salinity in alkaline conditions, we determined if J3 also has an effect on PM H⁺-ATPase activity. Plasma membrane-enriched vesicles were isolated from 5-week-old Col-0, *pks5-1*, *j3-1*, and *j3-2* plants treated with or without 250 mM NaCl for 3 or 6 d, and the ATP hydrolytic and H⁺-transport activities of the H⁺-ATPase were measured. Assays in the presence of specific H⁺-ATPase inhibitors demonstrated that the vesicles were enriched in plasma membranes and that they were transport competent (see Supplemental Table 1 and Supplemental Figure 8 online). Unless indicated, all PM H⁺-ATPase activity assays shown monitor the H⁺-transport activity of the H⁺-ATPase. Without NaCl treatment, there was no significant difference in PM H⁺-ATPase activity between Col-0 and the *j3* mutants (Figure 4A). After plants were treated with NaCl, PM H⁺-ATPase activity increased significantly in all plants. However, the increase in activity was significantly lower in the vesicles isolated from *j3* mutant plants compared with activity in Col-0 (Figures 4A to 4C). Consistent with previous results (Fuglsang et al., 2007), PM H⁺-ATPase activity in *pks5-1* mutant plants was higher than activity in Col-0 (Figures 4A to 4C). When we increased the time of treatment to 6 d, PM H⁺-ATPase activity increased further relative to activity after the 3-d treatment. The increase in Col-0 was 44%, but only 11% in *pks5-1*, 14% in *j3-1*, and 19% in *j3-2* mutants (Figures 4A and 4C). These results suggest that loss of either PKS5 or J3 in *Arabidopsis* alters regulation of PM H⁺-ATPase activity during salt stress. The difference in PM H⁺-ATPase activity between Col-0 and *j3* increased to 32% (*j3-1*) and 31% (*j3-2*) after 6 d of treatment compared with 14% (*j3-1*) and 16% (*j3-2*) after 3 d of treatment. Consistent with what we have shown previously, the pH optimum for PM H⁺-ATPase activity in *pks5-1* shifted from 6.5 to 7.0, while for *j3* mutants, the optimum stayed at 6.5, the same as for Col-0, but with lower activity (Figure 4D).

Addition of recombinant PKS5 protein to plasma membrane vesicles isolated from the *pks5-1* mutant rescued PM H⁺-ATPase activity to Col-0 levels (Fuglsang et al., 2007). To determine if addition of J3 protein in the assay also affects PM H⁺-ATPase activity, the *J3* coding region was cloned into the pGEX-6p-1 vector to generate a translational fusion to glutathione S-transferase (GST). The resulting plasmid was transferred into *E. coli* BL21 (DE3), and the J3 protein was purified and added to PM H⁺-ATPase assays. In the presence of 250 ng/mL J3, PM H⁺-ATPase activity increased in vesicles isolated from Col-0 and the *j3* mutant (Figures 4E and 4F). As a control, GST or boiled J3 protein was added to assays and did not have any effect on PM H⁺-ATPase activity (see Supplemental Figure 9 online). When we monitored the level of PM H⁺-ATPase protein in response to NaCl

treatment with immunoblot analysis using PM H⁺-ATPase antibodies, we did not observe significant differences in protein levels among Col-0, *pks5-1*, *j3-1*, and *j3-2* plants (see Supplemental Figures 10A and 10B online). Addition of J3 protein to membranes isolated from *pks5-1* had no significant effect on activity (Figures 4E and 4F). These data indicate that J3 is a novel regulator of PM H⁺-ATPase activity and that this regulation likely takes place via mediation of PKS5 activity.

Proton Efflux Is Increased in Roots of *pks5-1* and Decreased in Roots of *j3* Mutants

Previously, we have shown that the rate of proton secretion in roots of *pks5-1* plants is higher than that in wild type in alkaline conditions (Fuglsang et al., 2007). The *j3* mutants have opposite phenotypes in terms of PM H⁺ ATPase activity, sensitivity to salt, and alkalization when compared with *pks5-1* plants. To determine the effect of salt and alkaline conditions on in vivo proton fluxes in the root of *j3* seedlings, we used the pH-sensitive ratiometric probe D-1950, a dextran-conjugated membrane impermeable fluorescence dye that reports pH changes between pH 5.0 and pH 8, to measure proton secretion in the upper region of the root and used microelectrode ion flux estimation (MIFE) assays for proton efflux measurements at the root apex (as described in Fuglsang et al., 2007).

Seven-day-old seedlings of Col-0, *pks5-1*, *j3-1*, and *j3-2* grown on medium at pH 5.8 were preincubated with D1950 (20 μM) in a buffer containing 10 mM KCl at pH 6.0. The probe was found in the apoplast but not in the cytoplasm (Figures 5A to 5C). The seedlings were subsequently treated with KHCO₃ buffer, pH 8.4, containing 75 mM NaCl. A pH increase was detected immediately, and a decrease in apoplast pH in the root was seen as a fluorescence change by confocal microscopy. Consistent with previous findings, the pH in the apoplast of roots in the *pks5-1* mutant decreased faster than in Col-0 in response to salt in alkaline conditions, suggesting that the *pks5-1* mutant secretes more H⁺ into the apoplast. However, the rate of decrease in the *j3* mutants was largely reduced compared with Col-0, suggesting that the *j3* mutant secretes less H⁺ into the apoplast (Figure 5E).

For noninvasive ion flux measurements, net H⁺ fluxes were measured in the root apex of 7-d-old seedlings of Col-0, *pks5-1*, *j3-1*, and *j3-2*. The seedlings were preincubated in buffer (0.5 mM KCl, 0.1 mM CaCl₂, and 0.3 mM MES, pH 6.0) for 20 min and assayed in the same buffer containing 75 mM NaCl at pH 7.7. The transmembrane H⁺ efflux increased in *pks5-1* and decreased in *j3* compared with Col-0 (Figures 5F and 5G). To determine if the changes in H⁺ efflux in the mutants are due to the changes in PM H⁺-ATPase activity, net H⁺ fluxes at the root apex of Col-0 and

Figure 5. (continued).

(H) Vanadate treatment eliminated the net proton effluxes. The seedlings of Col-0, *pks5-1*, *j3-1*, and *j3-2* were treated with alkaline conditions (pH 7.7) plus 75 mM NaCl and 1 mM vanadate and then the net proton effluxes were measured.

(I) Calculated net proton effluxes from **(H)**. A Student's *t* test was used to determine statistical significance; significant differences ($P \leq 0.05$) in **(G)** and **(I)** are indicated by different lowercase letters.

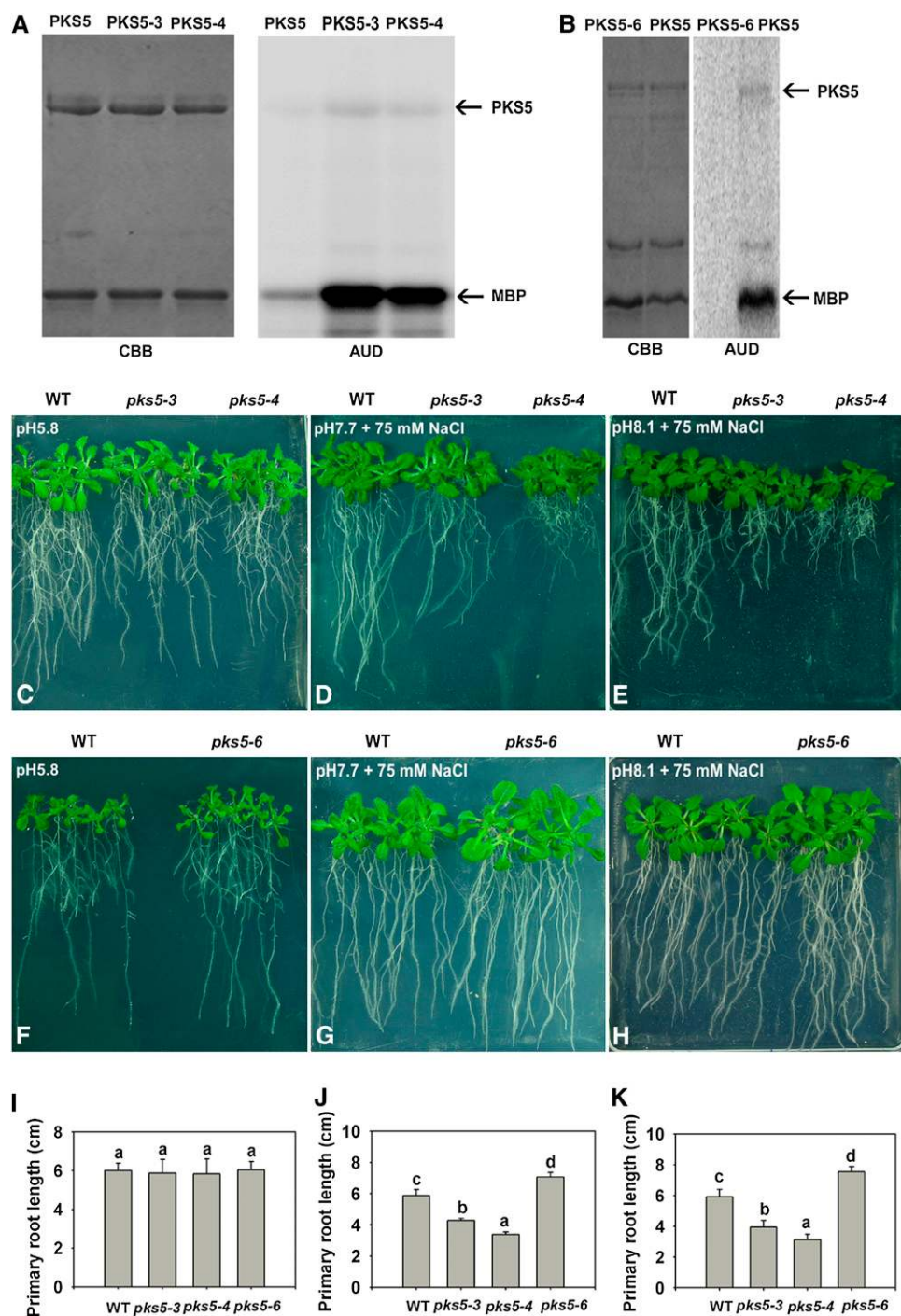


Figure 6. PKS5 Kinase Activity Negatively Correlates with PM H⁺-ATPase Activity and Seedling Sensitivity to Salt in Alkaline Conditions.

(A) and **(B)** Kinase activity comparison for the PKS5, PKS5-3, PKS5-4, and PKS5-6 proteins. Left panel: Coomassie blue (CBB)-stained SDS-PAGE gel containing the PKS5 wild-type and mutant proteins and the substrate, MBP. Right panel: autoradiograph (AUD) of kinase activity assays shown in the left panel.

(C) to **(H)** Five-day-old wild type (*Col er105*), *pks5-3*, *pks5-4*, and *pks5-6* seedlings grown on MS medium at pH 5.8 were transferred to MS medium at pH 5.8, at pH 7.7 with 75 mM NaCl, or at pH 8.1 with 75 mM NaCl. Photographs in **(C)** and **(F)** were taken 7 d after transfer; in **(D)** and **(G)**, 14 d after transfer; and in **(E)** and **(H)**, 21 d after transfer.

(I) Primary root elongation of seedlings transferred to MS medium at pH 5.8.

(J) Primary root elongation of seedlings transferred to MS medium at pH 7.7 with 75 mM NaCl.

(K) Primary root elongation of seedlings transferred to MS medium at pH 8.1 with 75 mM NaCl.

In **(I)** to **(K)**, primary root length was measured 7, 14, and 21 d after transfer, respectively. Error bars represent SD (plant number >15). A Student's *t* test was used for determining the statistical significance; significant differences ($P \leq 0.05$) in **(I)** to **(K)** are indicated by different lowercase letters.

[See online article for color version of this figure.]

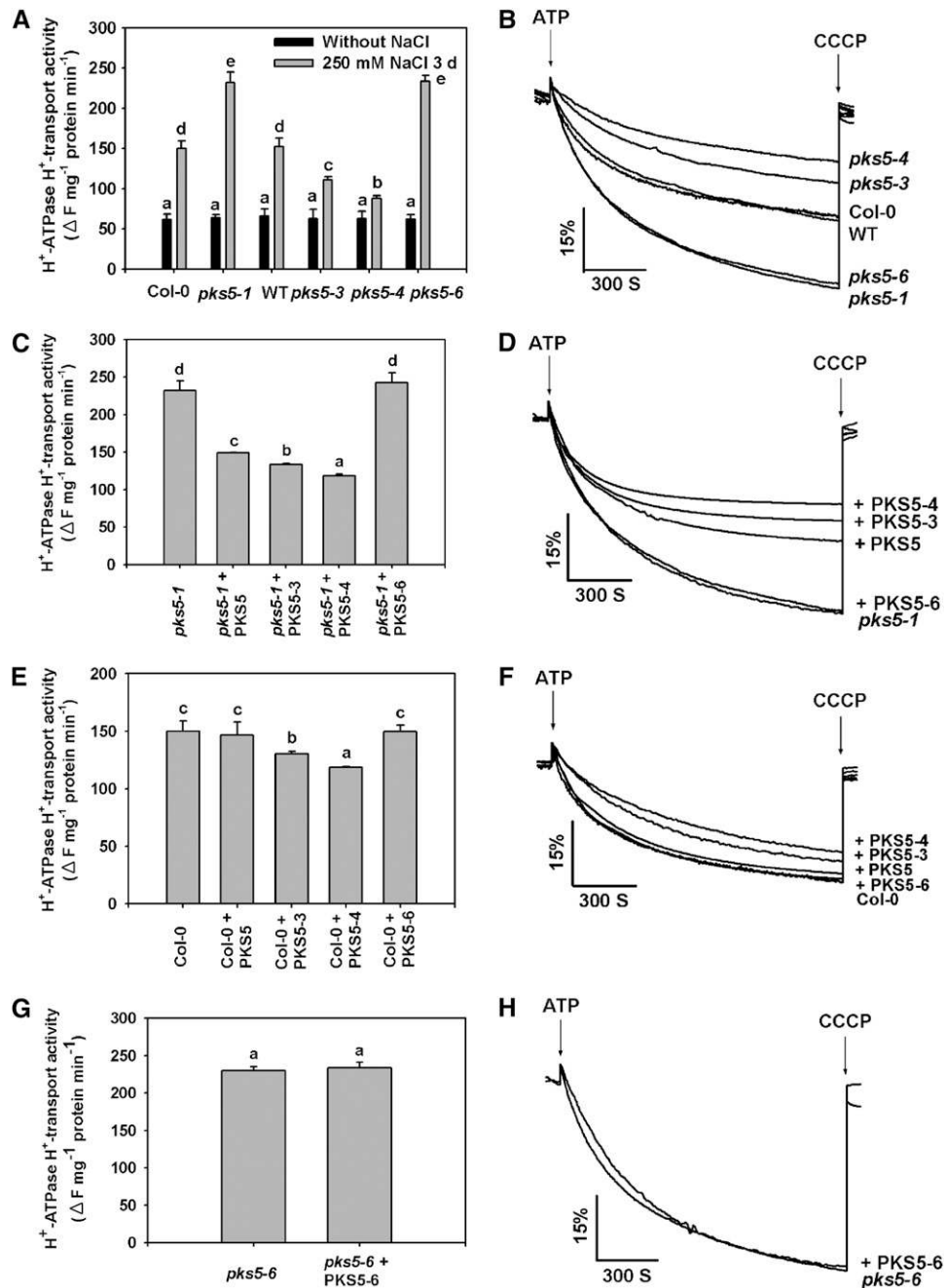


Figure 7. PK5 Inhibits PM H⁺-ATPase Activity.

PM vesicles were isolated from wild-type (*Col er105*), Col-0, *pks5-1* T-DNA insertion, and *pks5-3*, *pks5-4*, and *pks5-6* point mutant plants treated with or without 250 mM NaCl for 3 d. PM H⁺-ATPase activity (H⁺-transport) was initiated by addition of 3 mM ATP, and the pH gradient was collapsed by addition of 10 μM CCCP. PM H⁺-ATPase activity was measured in the vesicles as follows.

(A) Comparison of PM H⁺-ATPase activity in vesicles isolated from Col-0, *pks5-1*, wild-type, *pks5-3*, *pks5-4*, and *pks5-6* plants treated with or without 250 mM NaCl for 3 d.

(B) PM H⁺-ATPase activity was determined in the vesicles isolated from Col-0, *pks5-1*, wild-type, *pks5-3*, *pks5-4*, and *pks5-6* plants treated with 250 mM NaCl for 3 d.

(C) Comparison of PM H⁺-ATPase activity in vesicles isolated from *pks5-1* mutant plants in the presence of 250 ng/mL PKS5, PKS5-3, PKS5-4, or PKS5-6 recombinant protein.

(D) PM H⁺-ATPase activity was measured in the vesicles isolated from *pks5-1* mutant plants in the presence of 250 ng/mL PKS5, PKS5-3, PKS5-4, or PKS5-6 recombinant protein.

the mutants were measured in pH 7.7 buffer containing 1 mM vanadate, an inhibitor of P-type ATPases (Figures 5H and 5I). No difference in net H⁺ efflux was detected for Col-0, *pk5-1*, *j3-1*, or *j3-2*, and vanadate eliminated H⁺ extrusion in all plants tested. Taken together, our results suggest that PM H⁺-ATPase activity is a major factor contributing to the higher rate of proton secretion in the *pk5-1* root and the lower rate in *j3* mutants in salt and alkaline conditions.

PKS5 Activity Negatively Correlates with PM H⁺-ATPase Activity and Seedling Sensitivity to Salt in Alkaline Conditions

To further demonstrate that J3 regulates PM H⁺-ATPase activity by mediating PKS5 kinase activity, we isolated *pk5* mutants with differing levels of kinase activity. To do this, we screened a tilling (targeting-induced local lesions in genomes) mutant pool (Till et al., 2003) and isolated three *pk5* point mutation alleles. Tilling mutants were generated in the Col *er105* genetic background (Torii et al., 1996), hereafter referred to as the wild type. We backcrossed the mutants three times into Col-0. These mutations are distributed throughout the protein, including in the N-terminal kinase domain (*pk5-4*) and in the C-terminal regulatory domain (*pk5-3*) (see Supplemental Figure 11 online). In the *pk5-3* mutant, the Ser at position 317 in the FISL motif was mutated to Leu; in the *pk5-4* mutant, the Ala at position 168 in the kinase activation loop was mutated to Val; while in the *pk5-6* mutant, the Gly at position 219 in the kinase domain was mutated to Ser (see Supplemental Figure 11 online). Both the kinase activation loop and the FISL motif have been shown to be important for PKS activity (Guo et al., 2001). We first tested whether these mutations affect PKS5 activity. PKS5 cDNAs were amplified from Col-0 and *pk5* mutants and cloned into the pQE30 vector containing a HIS tag. The fusion proteins were purified from *E. coli* using His affinity chromatography, and the purified PKS5 proteins were used in kinase assays. PKS5 has been shown to be an active kinase in both auto- and trans-(substrate) phosphorylation (Fuglsang et al., 2007). When compared with the activity of the wild-type PKS5 protein, recombinant PKS5-3 and PKS5-4 proteins were more active; however, PKS5-6 was less active in both autophosphorylation and Myelin Basic Protein (MBP) phosphorylation (Figures 6A and 6B; see Supplemental Figure 12 online).

Next we tested the NaCl sensitivity of the *pk5* mutants at alkaline pH. Five-day-old wild-type, *pk5-3*, *pk5-4*, and *pk5-6* seedlings grown on medium at pH 5.8 were transferred to medium at pH 5.8, pH 7.7 with 75 mM NaCl, or pH 8.1 with 75 mM NaCl. No significant growth differences were detected between the wild type and *pk5* mutants on medium at pH 5.8 (Figures 6C, 6F, and 6I; see Supplemental Figure 13A online). On medium at pH 7.7 with NaCl, root growth of *pk5-3* and *pk5-4* (which had proteins with higher kinase activity than the wild-type PKS5 protein) was significantly reduced compared with the wild type (Figures 6D and 6J; see Supplemental Figure 13B online). Root elongation in the *pk5-3* and *pk5-4* mutants was reduced compared with that in wild type, and this reduction in growth was even more pronounced at pH 8.1 in the presence of 75 mM NaCl (Figures 6E and 6K; see Supplemental Figure 13C online). However, the root growth of *pk5-6* (which had protein with much lower kinase activity than the wild-type PKS5 protein) was significantly greater than the growth of the wild type (Figures 6G, 6H, 6J, and 6K). These results demonstrate that PKS5 activity negatively correlates with root growth on media with salt at alkaline pH.

Our previous data suggested that PKS5 is a negative regulator of the PM H⁺-ATPase (Fuglsang et al., 2007). To further demonstrate the link between PKS5 kinase and PM H⁺-ATPase activities, plasma membrane vesicles were isolated from leaves of Col-0, wild-type, *pk5-1*, *pk5-3*, *pk5-4*, and *pk5-6* plants treated with or without 250 mM NaCl, and PM H⁺-ATPase activity was measured. Without NaCl treatment, Col-0, the wild type, and the mutants had similar levels of PM H⁺-ATPase activity, and salt stress increased their activity but to different levels (Figures 7A and 7B). Consistent with previous observations, PM H⁺-ATPase activity (quenching of fluorescence) was much higher in vesicles isolated from *pk5-1* than in vesicles isolated from Col-0 (Figures 7A and 7B). Similar results were observed with vesicles isolated from the *pk5-6* mutant. PM H⁺-ATPase activity in vesicles isolated from the *pk5-3* and *pk5-4* mutants was much lower than that of the wild type (Figures 7A and 7B). These results provide further support for a negative correlation between PM H⁺-ATPase activity and PKS5 kinase activity.

To provide additional evidence that changes in PM H⁺-ATPase activity in the *pk5* mutants are due to changes in PKS5 kinase activity, we added recombinant PKS5 proteins to transport assays with plasma membrane vesicles isolated from the *pk5-1*

Figure 7. (continued).

(E) Comparison of PM H⁺-ATPase activity in vesicles isolated from wild-type plants in the presence of 250 ng/mL PKS5, PKS5-3, PKS5-4, or PKS5-6 recombinant protein.

(F) PM H⁺-ATPase activity was measured in vesicles isolated from wild-type plants in the presence of 250 ng/mL PKS5, PKS5-3, PKS5-4, or PKS5-6 recombinant protein.

(G) Comparison of PM H⁺-ATPase activity in vesicles isolated from *pk5-6* mutant plants in the presence of 250 ng/mL of recombinant PKS5-6 protein.

(H) The PM H⁺-ATPase activity was measured in the vesicles isolated from *pk5-6* mutant plants in the presence of 250 ng/mL PKS5-6 recombinant protein.

The units of the PM H⁺-ATPase activity are ΔF/min per mg protein. All data represent means ± SE of at least three replicate experiments. Each replicate was performed using independent membrane preparations. One representative experiment of three replicates is shown in **(B)**, **(D)**, **(F)**, and **(H)**. A Student's *t* test was used to determine statistical significance; significant differences (*P* ≤ 0.05) in **(A)**, **(C)**, **(E)**, and **(G)** are indicated by different lowercase letters.

mutant. Consistent with previous studies, wild-type PKS5 protein significantly reduced PM H⁺-ATPase activity in vesicles isolated from the *pks5-1* mutant (Figures 7C and 7D) and had no effect on the PM H⁺-ATPase activity of vesicles isolated from Col-0 plants (Figures 7E and 7F). Recombinant PKS5-6 protein had no effect on PM H⁺-ATPase activity in the vesicles isolated from Col-0 or the *pks5-1* and *pks5-6* mutants (Figures 7C to 7H). When either PKS5-3 or PKS5-4 protein was added to vesicles isolated from Col-0 or the *pks5-1* mutant, PM H⁺-ATPase activity was reduced; however, this effect was much more dramatic in *pks5-1* compared with Col-0 (Figures 7C to 7F). When used as controls, boiled recombinant PKS recombinant proteins did not have any effect on PM H⁺-ATPase activity. These results support the conclusion that PKS5 kinase activity is negatively correlated with PM H⁺-ATPase activity.

J3 Functions Upstream of PKS5 in the Regulation of PM H⁺-ATPase Activity

To determine whether *PKS5* genetically interacts with *J3*, we crossed *j3-1* to *pks5-1*, *pks5-3*, or *pks5-4* to generate *j3-1 pks5-1*, *j3-1 pks5-3*, and *j3-1 pks5-4* double mutants. T-DNA insertions in *pks5-1* and *j3-1* were confirmed using gene-specific primers, and the *pks5-3* and *pks5-4* mutations were confirmed using derived cleaved amplified polymorphic sequences (dCAPS) primer-based PCR followed by sequencing of the mutations. To assay PM H⁺-ATPase activity, plasma membrane-enriched vesicles were isolated from Col-0 and double mutant plants treated with or without 250 mM NaCl. As shown in Figure 8, the PM H⁺-ATPase activity of the salt-treated *j3-1 pks5-1* double mutant was similar to the activity of the *pks5-1* single mutant, and the activities of both were higher than the activity in Col-0 after salt treatment. These results indicate that, genetically, *J3* functions upstream of *PKS5*. Furthermore, PM H⁺-ATPase activity in both the *j3-1 pks5-3* and *j3-1 pks5-4* double mutants was similar to the activity of their respective *pks5* parent and lower than that of the *j3-1* parent (Figure 8). These results demonstrate that *J3* regulates PM H⁺-ATPase activity by mediating *PKS5* kinase activity.

To determine if the altered PM H⁺-ATPase activity in the double mutants correlates with seedling responses to salt in alkaline conditions, 5-d-old *j3-1*, *pks5-1*, *j3-1 pks5-1*, *pks5-3*, *j3-1 pks5-3*, *pks5-4*, and *j3-1 pks5-4* plants grown on medium at pH 5.8 were transferred to MS medium at pH 5.8, pH 7.7 with 75 mM NaCl, or pH 8.1 with 75 mM NaCl. Consistent with measurements of PM H⁺-ATPase activity, all of the double mutants showed phenotypes similar to their *pks5* parent (Figure 9; see Supplemental Figure 14 online), suggesting that *J3* regulates PM H⁺-ATPase activity and plant response to salt at alkaline pH by mediating *PKS5* activity.

J3 Represses *PKS5* Kinase Activity

Our results demonstrate that *J3* interacts with and functions genetically upstream of *PKS5*. In addition, these proteins have opposite effects on the regulation of PM H⁺-ATPase activity and seedling sensitivity to salt at alkaline pH. One explanation for these observations is *J3* represses *PKS5* kinase activity. To test

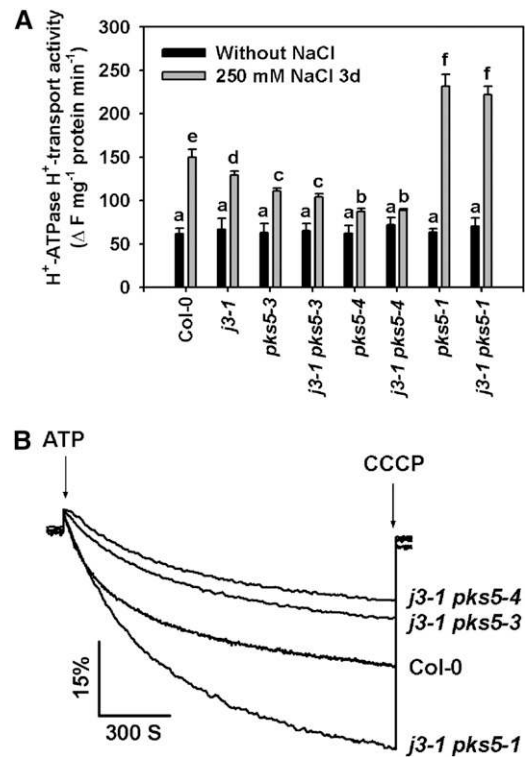


Figure 8. *J3* Regulates PM H⁺-ATPase Activity through *PKS5*.

Plasma membrane vesicles were isolated from Col-0, *j3-1 pks5-1*, *j3-1 pks5-3*, and *j3-1 pks5-4* mutant plants treated with or without 250 mM NaCl for 3 d. PM H⁺-ATPase activity was initiated by addition of 3 mM ATP, and the pH gradient was collapsed by addition of 10 μM CCCP. PM H⁺-ATPase activity was measured in the vesicles as follows.

(A) Comparison of PM H⁺-ATPase activity in vesicles isolated from Col-0, *j3-1*, *pks5-3*, *j3-1 pks5-3*, *pks5-4*, *j3-1 pks5-4*, *pks5-1*, and *j3-1 pks5-1* plants treated with or without 250 mM NaCl for 3 d.

(B) PM H⁺-ATPase activity was determined in vesicles isolated from Col-0, *j3-1 pks5-1*, *j3-1 pks5-3*, and *j3-1 pks5-4* plants treated with 250 mM NaCl for 3 d.

The units of PM H⁺-ATPase activity are ΔF/min per mg protein. All data represent means ± SE of at least three replicate experiments. Each replicate was performed using independent membrane preparations. One representative experiment of three replicates is shown in **(B)**. A Student's *t* test was used to determine statistical significance; significant differences ($P \leq 0.05$) in **(A)** are indicated by different lowercase letters.

this hypothesis, a protein kinase assay was performed. As predicted, *J3* repressed *PKS5* kinase activity (Figures 10A to 10C and 10E), and the more *J3* protein that was added to the reaction, the more *PKS5* activity was inhibited. The specificity of this repression was shown based on the lack of *J3* repression of the kinase activity of *SOS2* (Figures 10D and 10E), a *PKS5* homolog.

When we overexpressed *J3* in the *pks5-1* and *pks5-3* mutants, the *pks5-3* salt sensitive phenotype in alkaline conditions was rescued, whereas the phenotype of *pks5-1* was not significantly altered (Figures 10F to 10S; see Supplemental Figure 15 online). These results further support the conclusion that *J3* regulation of

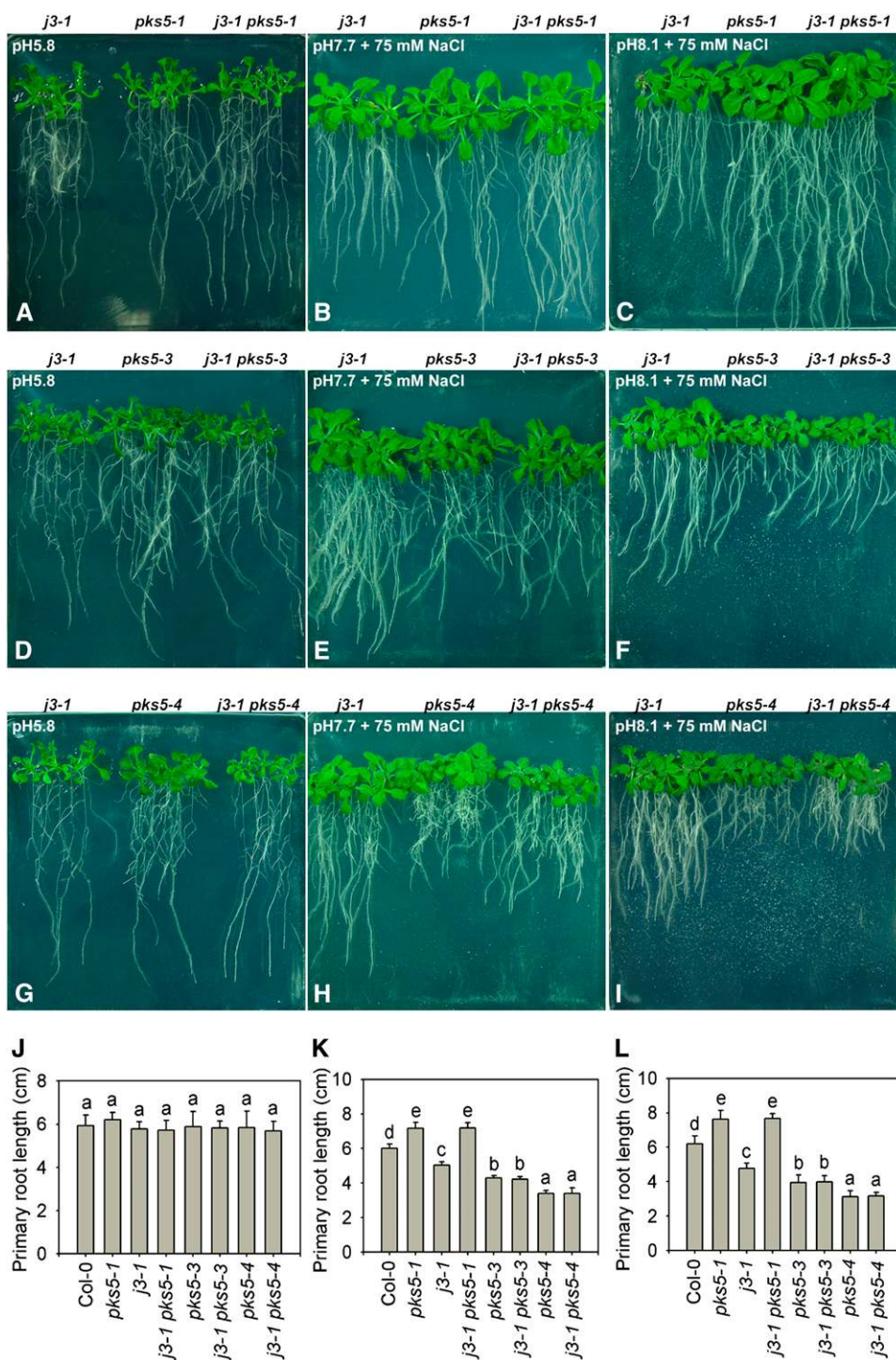


Figure 9. The *j3-1 pks5* Double Mutants Phenocopy the *pks5* Response to Salt in Alkaline Conditions.

(A) to (I) Five-day-old *j3-1*, *pks5-1*, *j3-1 pks5-1*, *pks5-3*, *j3-1 pks5-3*, *pks5-4*, and *j3-1 pks5-4* mutant seedlings grown on MS medium at pH 5.8, at pH 7.7 with 75 mM NaCl, or at pH 8.1 with 75 mM NaCl. Photographs in **(A)**, **(D)**, and **(G)** were taken 7 d after transfer; in **(B)**, **(E)**, and **(H)**, 14 d after transfer; and in **(C)**, **(F)**, and **(I)**, 21 d after transfer.

(J) Primary root elongation of plants transferred to MS medium at pH 5.8.

(K) Primary root elongation of plants transferred to MS medium at pH 7.7 with 75 mM NaCl.

(L) Primary root elongation of plants transferred to MS medium at pH 8.1 with 75 mM NaCl.

In **(J)** to **(L)**, primary root length was measured 7, 14, and 21 d after transfer, respectively. Error bars represent SD (plant number >15). A Student's *t* test was used to determine statistical significance; significant differences ($P \leq 0.05$) in **(J)** to **(L)** are indicated by different lowercase letters.

[See online article for color version of this figure.]

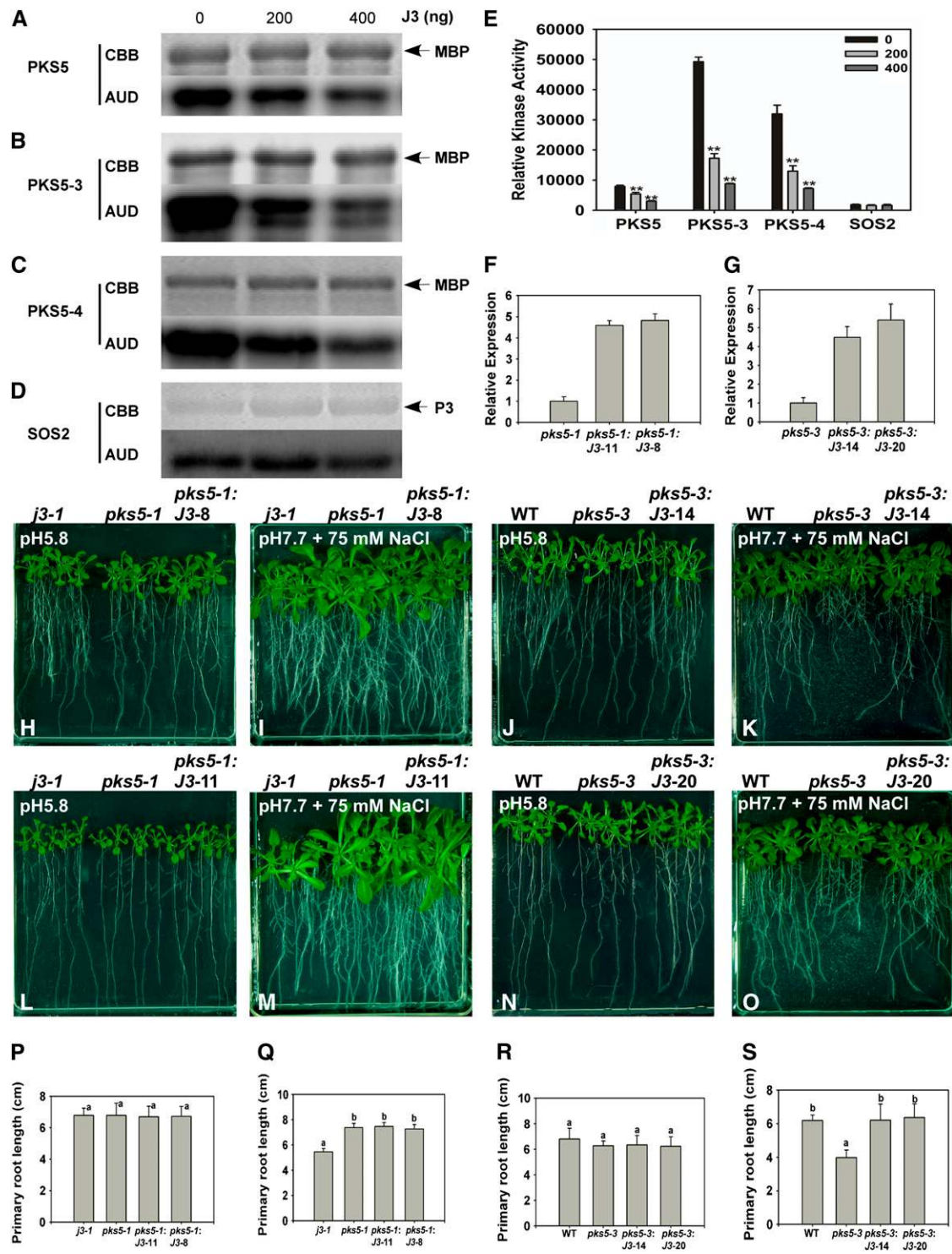


Figure 10. J3 Represses PKS5 Kinase Activity.

Increasing concentrations of J3 protein were incubated in kinase assay buffer with PKS5 (A), PKS5-3 (B), PKS5-4 (C), or SOS2 (D) protein. Top panel: SDS-PAGE gel with MBP or GST-P3 stained with Coomassie blue (CBB). Lower panel: MBP or GST-P3 (P3; a synthetic peptide designed based on the recognition sequences of protein kinase C or SNF1/AMPK kinases, ALARAASAAALARRR) substrate phosphorylation (AUD).

(E) Quantification of data shown in (A) to (D).

(F) and (G) Overexpression of J3 in *pks5-1* and *pks5-3* mutants. Total RNA was extracted from 12-d-old seedlings of *pks5-1*, *pks5-3*, and

the response of the plant to salt in alkaline conditions takes place via repression of PKS5 kinase activity.

DISCUSSION

The PM H⁺-ATPase is a highly regulated enzyme with numerous physiological functions (Dubey et al., 2009). Evidence exists for changes in phosphorylation status of the H⁺-ATPase leading to either activation or inhibition of enzyme activity (Vera-Estrella et al., 1994; Xing et al., 1996; Schaller and Oecking, 1999). Activation of the enzyme requires phosphorylation of its C terminus leading to the binding of 14-3-3 proteins and the removal of an autoinhibition by the R domain. Several phosphorylation sites have been identified in the C-terminal region of the protein (Dubey et al., 2009). While little is known about the protein kinases or phosphatases that are directly responsible for altering PM H⁺-ATPase phosphorylation status, several proteins have been implicated in the C-terminal phosphorylation events leading to binding of the regulatory 14-3-3 protein (Xing et al., 1996; Lino et al., 1998; Svennelid et al., 1999; Fuglsang et al., 2006).

PKS5 was identified as a protein that negatively regulates PM H⁺-ATPase activity and controls intracellular pH homeostasis in response to alkaline pH (Fuglsang et al., 2007). PKS5 phosphorylates Ser-931 on the AHA2 isoform of the PM H⁺-ATPase, which, in turn, blocks interaction between AHA2 and an activating 14-3-3 protein. Phosphorylation of this residue is independent of Thr-947 phosphorylation of AHA2 (Fuglsang et al., 2007). In the tobacco PMA2 isoform, the corresponding residue (Ser-938) is phosphorylated in vivo (Dubey et al., 2009), although it is not known whether a SOS2-like protein kinase is involved in this event.

In this study, we identified a component in the PKS5 signaling pathway. J3 shares similar patterns of tissue-specific expression and subcellular localization with PKS5 and interacts with PKS5 in planta (Figures 1 and 2). However, *j3* knockout mutants display the opposite phenotype from *pks5* loss-of-function mutants, with the *j3* mutants displaying increased sensitivity to NaCl at alkaline pH and decreased PM H⁺-ATPase activity (Figures 3 and 4). Double mutant analysis suggests that J3 relies on and functions upstream of PKS5. Overexpression of *J3* rescues the *pks5-3* (a PKS5 constitutively active mutant) salt-sensitive phenotype in alkaline conditions but does not alter *pks5-1* (a PKS5 T-DNA knockout mutant) phenotype (Figure 10). These findings are consistent with the observation that J3 represses PKS5 kinase

activity (Figures 8 to 10). Interestingly, *j3-1 pks5-3* and *j3-1 pks5-4* double mutants have similar levels of PM H⁺-ATPase activity and similar sensitivity to growth in media with NaCl at alkaline pH to what is seen for their *pks5* parent (Figures 8 and 9). The fact that the phenotypes in these double mutants are not more severe suggests that other, as yet unidentified, components may also be involved in the regulation of phosphorylation/dephosphorylation of Ser-931 and that there is a threshold effect of PKS5 kinase activity on the regulation of PM H⁺-ATPase activity.

PM H⁺-ATPase activity is stimulated by many environmental changes, known to be regulated by a calcium-dependent ScaBP1-PKS5 pathway. When the *Arabidopsis* proteins are expressed in yeast, repression of PM H⁺-ATPase activity by PKS5 is dependent on the presence of ScaBP1 (Fuglsang et al., 2007); however, it is currently not known how ScaBP1 regulates the PKS5 protein. The predicted functions of the ScaBP proteins are to perceive changes in intracellular calcium levels (calcium sensors) and then to interact with, activate, and recruit PKS kinase proteins to cell membranes to activate their targets (Halfter et al., 2000; Quintero et al., 2002; Xu et al., 2006; Fuglsang et al., 2007; Quan et al., 2007; Lin et al., 2009). It has been shown that ANJ1, a DnaJ-like protein in *Atriplex nummularia*, is farnesylated and geranylgeranylated in planta (Zhu et al., 1993). These modifications rely on a Cys in the CAQQ motif at the C terminus of the ANJ1 protein and increase the association of ANJ1 with the cell membrane (Zhu et al., 1993). This CAQQ motif is absolutely conserved in the J3 C terminus, suggesting that, during growth in NaCl at alkaline pH, J3 is prenylated and this leads to the localization of J3 to the plasma membrane and to activation of PM H⁺-ATPase via inhibition of PKS5 or, alternatively, by modifying the affinity of PKS5 for the H⁺-ATPase.

In summary, we identified a new component of the PKS5 signal transduction pathway that positively regulates PM H⁺-ATPase activity in *Arabidopsis*. Our work provides additional evidence that regulation of the phosphorylation status of the PM H⁺-ATPase is critical for the response of *Arabidopsis* to environmental stimuli.

METHODS

Plant Materials

Plants were grown in controlled growth chambers under a 16-h-light (22°C)/8-h-dark (20°C) cycle. The following *Arabidopsis thaliana* strains were used in this study: Col-0 and Col *erecta105* (wild type), which was

Figure 10. (continued).

overexpression *J3* transgenic plants in both the *pks5-1* and *pks5-3* background. The resulting cDNAs were used for real-time PCR analysis. Error bars indicate SD ($n = 3$).

(H) to **(O)** Five-day-old *pks5-1*, *pks5-3*, wild-type, Col-0 seedlings, and seedlings overexpressing *J3* in *pks5-1* and *pks5-3* grown on MS medium at pH 5.8 were transferred to MS medium at pH 5.8 or at pH 7.7 with 75 mM NaCl. Photographs in **(H)**, **(J)**, **(L)**, and **(N)** were taken 7 d after transfer; in **(I)**, **(K)**, **(M)**, and **(O)**, 14 d after transfer.

(P) and **(R)** Primary root elongation of seedlings transferred to MS medium at pH 5.8.

(Q) and **(S)** Primary root elongation of seedlings transferred to MS medium at pH 7.7 with 75 mM NaCl.

Primary root length was measured 7 d after transfer in **(H)**, **(J)**, **(L)**, and **(N)** and 14 d after transfer in **(I)**, **(K)**, **(M)**, and **(O)**. Error bars represent SD (plant number >15). A Student's *t* test was used for determining the statistical significance; significant differences ($P \leq 0.05$) in **(P)** to **(S)** are indicated by different lowercase letters.

[See online article for color version of this figure.]

used for generating Tilling mutants. For salt treatment, 5-week-old plants were treated with or without 250 mM NaCl for 3 or 6 d. The Tilling mutants (Till et al., 2003) *pks5-3*, *pks5-4*, and *pks5-6* were obtained from the ABRC (Alonso et al., 2003), and homozygous lines were identified by dCAPS-based PCR and sequencing. The following dCAPS primer sequences were used: *pks5-3*, 5'-GCGTTTGATTGATTTCTACTCCT-3' and 5'-CACCA-CAAGCAAATCATTCAA-3' were used to amplify a 263-bp DNA fragment with an *AvaI* site to distinguish *pks5-3* and the wild type; *pks5-4*, 5'-GTTTCGATTTCCGGTCTAAACG-3' and 5'-CTCTCCTTTATAAATC-TTC-3' harboring an *MluI* site were used to amplify a 236-bp DNA fragment; *pks5-6*, 5'-GTCTTGTTCGTTCTCGTCACC-3' and 5'-CTGATC-TTCGATCTCGTCATC-3' harboring an *AgeI* site were used to amplify a 252-bp fragment. *j3* T-DNA insertion mutants (SALK_132923 and SALK_141625) were obtained from ABRC and identified using the following primer sequences: 5'-GCTGTTGACGGCTTAGGTAG-3' or 5'-TTCGAC-TCGATCTTGGCGTTT-3' and left border T-DNA primers LBa1 5'-TGGTT-CACGTAGTGGGCCATCG-3' and LBb1 5'-GCGTGGACCGCTTCTGTC-CAACT-3'. *j3-1 pks5-1*, *j3-1 pks5-3*, and *j3-1 pks5-4* double mutants were obtained by crossing *j3-1* to *pks5-1*, *pks5-3*, and *pks5-4* respectively, and confirmed by PCR and sequencing.

Plasmid Construction

The full-length *PKS5* coding sequence was amplified by RT-PCR using 5'-CGGGATCCATGCCAGAGATCGAGATTGCC-3' and 5'-GGAATTC-TAAATAGCCGDTTGTG-3' primers harboring a *Bam*HI or *Eco*RI site, respectively. The PCR products were cloned into the pGEX-6p-1 vector between *Bam*HI and *Eco*RI sites. The coding sequences of *PKS5-3*, *PKS5-4*, and *PKS5-6* were also cloned into pGEX-6p-1. All fragments containing *PKS5* and mutant coding sequences were digested from pGEX-6p-1 with *Bam*HI and *SalI* and subcloned into pQE30 to generate fusions to a His-tag. *J3* was amplified using primers 5'-CGGGATC-CATGTTCCGGTAGAGGACCCTC-3' and 5'-GCGTCGACTTACTGCTGG-GCACATTGCA-3' and cloned into the *Bam*HI and *SalI* sites of pET28a. *J3* was then subcloned from this plasmid into other expression vectors as indicated. All plasmids were verified by sequencing.

Kinase Activity Assays

Fusion constructs were transformed into *Escherichia coli* strain BL21 (DE3). The recombinant proteins were purified with glutathione-Sepharose (Amersham Pharmacia) according to the manufacturer's protocol. Kinase activity assays were started by mixing 100 ng of the kinase and 500 ng of MBP in 20- μ L reactions with kinase assay buffer (20 mM Tris-HCl, pH 7.2, 5 mM MgCl₂, 0.5 mM CaCl₂, 10 μ M ATP, and 2 mM DTT). After addition of 0.3 μ L of [γ -³²P]ATP, the mixture was incubated at 30°C for 30 min. The reaction was terminated by the addition of 4 μ L of 5 \times SDS loading buffer, and the products were separated on 12% SDS-PAGE gels. The gels were stained with Coomassie Brilliant Blue, exposed on a storage phosphor screen, and phosphorylation visualized using a Typhoon 9410 phosphor imager (Amersham).

Yeast Two-Hybrid Assays

The *PKS5* coding sequence was cloned into the pAS2 vector between the *NcoI* and *SalI* sites. *PKS5N*, encoding the N-terminal 281 amino acids of *PKS5*, and *PKS5C*, encoding the C-terminal 154 amino acids, were amplified by PCR and were also cloned between the *NcoI* and *SalI* sites of pAS2. The *J3* coding sequence was cloned into the pACT2 vector between the *Bam*HI and *XhoI* sites. Plasmid DNA (50 μ g total) from an *Arabidopsis* cDNA library (ABRC) was transformed into the yeast Y190 strain harboring the pAS2-*PKS5* plasmid. Yeast transformation and growth assays were performed as described in the Yeast Protocols Handbook (Clontech). Two positive clones were identified, and sequence analysis revealed that they are identical to At3g44110 (*J3*).

RNA Gel Blot Analysis of *j3* Null Alleles

Total RNA was isolated from 10-d-old seedlings of Col-0, *pks5-1*, *j3-1*, and *j3-2* mutants. RNA (15 μ g) from each sample was used for RNA gel blot analysis (Guo et al., 2001).

Confocal Images and Proton Efflux Measurements

GFP-*J3* was constructed by excising the *J3* open reading frame from a His-*J3* plasmid with *Bam*HI and *SalI* and cloning it into the pCambia1205-GFP binary vector downstream of *GFP*. The coding sequences of *PKS5*, *PKS5-3*, *PKS5-4*, and *PKS5-6* were introduced into the pTA7002 vector after PCR amplification with the primers 5'-CCGCTCGAGATGCCA-GAGATCGAGATTGCC-3' and 5'-CCGCTCGAGAATAGCCGCGTTTGTG-GAC-3', which introduced *XhoI* restriction sites at each end. These constructs were transformed into Col-0 plants. Five-day-old transgenic T2 GFP-*J3* lines were used for subcellular localization. Five-day-old T2 pTA7002-*PKS5-YFP* transgenic plants were treated with 10 mM dexamethasone (Sigma-Aldrich) before analysis. GFP-*J3* and *PKS5-YFP* fluorescence was detected and images collected on a Zeiss 510 META confocal microscope. Proton efflux measurements and pH ratio imaging in the apoplast were as described (Fuglsang et al., 2007).

Promoter-GUS Analysis

A 1918-bp DNA fragment from -8 to -1926 bp upstream of the translational start site of *J3* was amplified with primers 5'-AGCGTCGACTGATT-GACGATGCTTTTAC-3' and 5'-CATGCCATGGCCGTTGTAACGAAA-ACCCTA-3' and cloned into the *NcoI* and *SalI* sites of the pCambia1301 vector. The plasmid was transformed into wild-type *Arabidopsis*, and transgenic T2 lines were used for GUS assays.

Quantitative Real-Time PCR

Total RNA was extracted with the TRI reagent (Ambion) from 10-d-old seedlings. Ten micrograms of total RNA was treated with RNase-free DNase I (Promega) to remove DNA, and 2 μ g of treated RNA was used for reverse transcription with M-MLV Reverse transcriptase (Promega) according to the manufacturer's protocol. Real-time PCR was performed using an ABI 7500 Fast Real-Time PCR instrument and SYBR Premix Ex Taq kit (TaKaRa). Gene expression levels were standardized using *ACTIN2* as an internal control. The following primer sequences were used: for *PKS5* expression, forward 5'-TCGTCGGGATTGGATTGTC-3' and reverse 5'-TCCATCTCAAACCCTACTC-3'; for *J3* expression, forward 5'-TTCTACCTAAGCCGTCAAC-3' and reverse 5'-CGTCATCAT-CATAAGCCTC-3'; for *ACTIN2*, forward 5'-GTCGTACAACCGGTA-TTGTG-3' and reverse 5'-GAGCTGGTCTTTGAGGTTTC-3'.

Coimmunoprecipitation

The plasmids were purified using a Plasmid Maxprep Kit (Vigorous Biotechnology) and introduced into *Arabidopsis* mesophyll protoplasts (Sheen, 2001). Coimmunoprecipitation was performed as described (Quan et al., 2007).

Plasma Membrane and Nuclei Isolation

Plasma membrane-enriched vesicles were isolated from 5-week-old plants using aqueous two-phase partitioning as described (Qiu et al., 2002). All steps were performed at 4°C or on ice. Plants were homogenized in isolation buffer containing 0.33 M sucrose, 10% (w/v) glycerol, 0.2% (w/v) BSA, 5 mM EDTA, 5 mM DTT, 5 mM ascorbate, 0.2% (w/v) casein, 0.6% (w/v) polyvinylpyrrolidone, 1 mM PMSF, 1 \times protease inhibitor, and 50 mM HEPES-KOH, pH 7.5. Two to four milliliters of homogenization buffer were used per gram of tissue. The homogenate

was filtered through two layers of Miracloth and centrifuged at 13,000g for 10 min. The supernatant then was centrifuged for 50 min at 80,000g to obtain a microsomal pellet that was resuspended in a buffer containing 0.33 M sucrose, 3 mM KCl, 0.1 mM EDTA, 1 mM DTT, 1 mM PMSF, 1× protease inhibitor, and 5 mM potassium phosphate, pH 7.8. The suspension was added to a phase mixture to obtain a phase system consisting of 6.2% (w/w) Dextran T-500 and 6.2% (w/w) polyethylene glycol 3350 in 5 mM potassium phosphate, pH 7.8, buffer containing 0.33 M sucrose and 3 mM KCl. The final upper phases were collected, diluted with resuspension buffer containing 0.33 M sucrose, 10% (w/v) glycerol, 0.1% (w/v) BSA, 0.1 mM EDTA, 2 mM DTT, 1× protease inhibitor, and 20 mM HEPES-KOH, pH 7.5, and centrifuged for 50 min at 100,000g. The resulting pellet was collected and resuspended with resuspension buffer containing 1 mM EDTA. Isolation of a nuclei-enriched fraction was performed as described (Bowler et al., 2004).

PM H⁺-ATPase Activity Assays

To characterize the activity of PM H⁺-ATPase, its H⁺-transport activity was measured as described (Qiu et al., 2002) using 50 μg of plasma membrane protein. When used, recombinant protein (250 ng/mL) was preincubated for 10 min at room temperature with plasma membrane vesicles. An inside-acid pH gradient (ΔpH) was formed in the vesicles by the activity of the H⁺-ATPase and measured as a decrease (quench) in the fluorescence of quinacrine (a pH-sensitive fluorescent probe). Assays (2 mL) contained 5 μM quinacrine, 3 mM MgSO₄, 100 mM KCl, 25 mM 1,3-bis[Tris(hydroxymethyl)methylamino]propane-HEPES, pH 6.5, 250 mM mannitol, and 50 μg/mL of plasma membrane protein. Reactions were mixed by inversion several times and then placed in a dark chamber in a fluorescence spectrophotometer (Hitachi F-4500). Reactions were equilibrated in the dark with stirring for 5 min before beginning fluorescence readings. The assay was initiated by the addition of ATP to a final concentration of 3 mM, and formation of ΔpH was measured at excitation and emission wavelengths of 430 and 500 nm, respectively. At the end of each reaction, 10 μM (final concentration) of the protonophore, m-chlorophenylhydrazine (CCCP) was added to dissipate any remaining pH gradient. Specific activity was calculated by dividing the change in fluorescence by the mass of plasma membrane protein in the reaction per unit time (ΔF/min per mg of protein). Unless indicated, all data represent means ± SE of at least three replicate experiments.

Determination of Plasma Membrane Purity

To characterize the membrane origin and purity of the membrane vesicles, H⁺-ATPase substrate hydrolytic activity was determined by measuring the release of P_i from ATP in the presence or absence of H⁺-ATPase specific inhibitors (Yan et al., 2002).

Accession Numbers

Sequence data from this article can be found in the Arabidopsis Genome Initiative under the following accession numbers: *PKS5*, At2g30360; *J3*, At3g44110.

Supplemental Data

The following materials are available in the online version of this article.

Supplemental Figure 1. Expression of *J3* and *PKS5* in Roots, Stems, Rosette Leaves, Cauline Leaves, Flowers, and Siliques Determined by Quantitative Real-Time PCR Using Gene-Specific Primers.

Supplemental Figure 2. Phenotypic Complementation of *j3-1* by Expression of 35SP:GFP-*J3*.

Supplemental Figure 3. Phenotypic Complementation of *pks5-1* by Expression of DexP:3×flag-*PKS5*.

Supplemental Figure 4. *PKS5* and *J3* Were Detected in Soluble and Plasma Membrane-Enriched Fractions.

Supplemental Figure 5. RT-PCR Analysis of *J3* in Col-0, *j3-1*, and *j3-2* Plants Using *ACTIN2* as Control.

Supplemental Figure 6. Alkaline Conditions Significantly Enhance *Arabidopsis* Sensitivity to Salt.

Supplemental Figure 7. Fresh Weight of Col-0, *pks5-1*, *j3-1*, and *j3-2* under Salt and Alkalinity Conditions.

Supplemental Figure 8. Vesicles Isolated from *Arabidopsis* Leaves Are Transport Competent.

Supplemental Figure 9. GST Protein Has No Effect on PM H⁺-ATPase Activity.

Supplemental Figure 10. Immunoblot of PM H⁺-ATPase Protein from Col-0, *pks5-1*, *j3-1*, and *j3-2* Plants.

Supplemental Figure 11. Schematic Diagram of Domains and *pks5* Point Mutations' Distribution in the *PKS5* Protein.

Supplemental Figure 12. Kinase Assay for Recombinant Proteins *PKS5*, *PKS5-3*, and pET28a Empty Vector.

Supplemental Figure 13. Fresh Weight of the Wild Type, *pks5-3*, *pks5-4*, and *pks5-6* under Salt and Alkalinity Conditions.

Supplemental Figure 14. Fresh Weight of Col-0, *j3-1*, *pks5-1*, *j3-1 pks5-1*, *pks5-3*, *j3-1 pks5-3*, *pks5-4*, and *j3-1 pks5-4* Seedlings under Salt and Alkalinity Conditions.

Supplemental Figure 15. Fresh Weight of *j3-1*, *pks5-1*, *pks5-3*, and *pks5-1 (pks5-1:J3)* or *pks5-3* Overexpressing *J3 (pks5-3:J3)* under Salt and Alkalinity Conditions.

Supplemental Table 1. Vesicles Isolated from *Arabidopsis* Leaves Are Enriched in Plasma Membranes.

ACKNOWLEDGMENTS

We thank Shidi Li and Jun Zhang for excellent technical assistance, Juan Sun and Lihua Hao from Xuyue (Beijing) Science and Technology for the MIFE assay, and the ABRC (Ohio State University) for the T-DNA insertion and Tilling lines. This work was supported by the National Basic Research Program of China (Grant 2006CB100100), the National High Technology Research and Development Program of China 863 (Grant 2008AA022304 to Y.G.), and U.S. Department of Energy/Energy Biosciences (Grant DE-FG02-04ER15616 to K.S.S.).

Received June 25, 2009; revised March 16, 2010; accepted March 30, 2010; published April 23, 2010.

REFERENCES

- Alonso, J.M., et al. (2003). Genome-wide insertional mutagenesis of *Arabidopsis thaliana*. *Science* **301**: 653–657.
- Aoyama, T., and Chua, N.H. (1997). A glucocorticoid-mediated transcriptional induction system in transgenic plants. *Plant J.* **11**: 605–612.
- Ayala, F., O'Leary, J.W., and Schumaker, K.S. (1996). Increased vacuolar and plasma membrane H⁺-ATPase activities in *Salicornia bigelovii* Torr. in response to NaCl. *J. Exp. Bot.* **47**: 25–32.

- Banecki, B., Liberek, K., Wall, D., Wawrzynów, A., Georgopoulos, C., Bertoli, E., Tanfani, F., and Zylicz, M. (1996). Structure-function analysis of the zinc finger region of the DnaJ molecular chaperone. *J. Biol. Chem.* **271**: 14840–14848.
- Boston, R.S., Viitanen, P.V., and Vierling, E. (1996). Molecular chaperones and protein folding in plants. *Plant Mol. Biol.* **32**: 191–222.
- Bowler, C., Benvenuto, G., Laflamme, P., Molino, D., Probst, A.V., Tariq, M., and Paszkowski, J. (2004). Chromatin techniques for plant cells. *Plant J.* **39**: 776–789.
- Brault, M., Amiar, Z., Pennarun, A.M., Monestiez, M., Zhang, Z., Cornel, D., Dellis, O., Knight, H., Bouteau, F., and Rona, J.P. (2004). Plasma membrane depolarization induced by abscisic acid in *Arabidopsis* suspension cells involves reduction of proton pumping in addition to anion channel activation, which are both Ca²⁺ dependent. *Plant Physiol.* **135**: 231–243.
- Bukau, B., and Horwich, A.L. (1998). The Hsp70 and Hsp60 chaperone machines. *Cell* **92**: 351–366.
- Camoni, L., Iori, V., Marra, M., and Aducci, P. (2000). Phosphorylation-dependent interaction between plant plasma membrane H⁺-ATPase and 14-3-3 proteins. *J. Biol. Chem.* **275**: 9919–9923.
- Caplan, A.J., Cyr, D.M., and Douglas, M.G. (1993). Eukaryotic homologues of *Escherichia coli* dnaJ: A diverse protein family that functions with hsp70 stress proteins. *Mol. Biol. Cell* **4**: 555–563.
- Duby, G., Poreba, W., Piotrowiak, D., Bobik, K., Derua, R., Waelkens, E., and Boutry, M. (2009). Activation of plant plasma membrane H⁺-ATPase by 14-3-3 proteins is negatively controlled by two phosphorylation sites within the H⁺-ATPase C-terminal region. *J. Biol. Chem.* **284**: 4213–4221.
- Fuglsang, A.T., Guo, Y., Cuin, T.A., Qiu, Q., Song, C., Kristiansen, K. A., Bych, K., Schulz, A., Shabala, S., Schumaker, K.S., Palmgren, M.G., and Zhu, J.K. (2007). *Arabidopsis* protein kinase PKS5 inhibits the plasma membrane H⁺-ATPase by preventing interaction with 14-3-3 protein. *Plant Cell* **19**: 1617–1634.
- Fuglsang, A.T., Tulinius, G., Cui, N., and Palmgren, M.G. (2006). Protein phosphatase 2A scaffolding subunit A interacts with plasma membrane H⁺-ATPase C-terminus in the same region as 14-3-3 protein. *Physiol. Plant.* **128**: 334–340.
- Georgopoulos, C.P., Lundquist-Heil, A., Yochem, J., and Feiss, M. (1980). Identification of the *E. coli* dnaJ gene product. *Mol. Gen. Genet.* **178**: 583–588.
- Gevaudant, F., Duby, G., von Stedingk, E., Zhao, R., Morsomme, P., and Boutry, M. (2007). Expression of a constitutively activated plasma membrane H⁺-ATPase alters plant development and increases salt tolerance. *Plant Physiol.* **144**: 1763–1776.
- Goffin, L., and Georgopoulos, C. (1998). Genetic and biochemical characterization of mutations affecting the carboxy-terminal domain of the *Escherichia coli* molecular chaperone DnaJ. *Mol. Microbiol.* **30**: 329–340.
- Guo, Y., Halfter, U., Ishitani, M., and Zhu, J.K. (2001). Molecular characterization of functional domains in the protein kinase SOS2 that is required for plant salt tolerance. *Plant Cell* **13**: 1383–1400.
- Halfter, U., Ishitani, M., and Zhu, J.K. (2000). The *Arabidopsis* SOS2 protein kinase physically interacts with and is activated by the calcium-binding protein SOS3. *Proc. Natl. Acad. Sci. USA* **97**: 3735–3740.
- Ham, B.K., Park, J.M., Lee, S.B., Kim, M.J., Lee, I.J., Kim, K.J., Kwon, C.S., and Paek, K.H. (2006). Tobacco Tsp1, a DnaJ-type Zn finger protein, is recruited to and potentiates Tsi1-mediated transcriptional activation. *Plant Cell* **18**: 2005–2020.
- Kanczewska, J., Marco, S., Vandermeeren, C., Maudoux, O., Rigaud, J.L., and Boutry, M. (2005). Activation of the plant plasma membrane H⁺-ATPase by phosphorylation and binding of 14-3-3 proteins converts a dimer into a hexamer. *Proc. Natl. Acad. Sci. USA* **102**: 11675–11680.
- Kim, Y.S., Min, J.K., Kim, D., and Jung, J. (2001). A soluble auxin-binding protein, ABP57. Purification with anti-bovine serum albumin antibody and characterization of its mechanistic role in the auxin effect on plant plasma membrane H⁺-ATPase. *J. Biol. Chem.* **276**: 10730–10736.
- Kinoshita, T., Nishimura, M., and Shimazaki, K. (1995). Cytosolic concentration of Ca²⁺ regulates the plasma membrane H⁺-ATPase in guard cells of fava bean. *Plant Cell* **7**: 1333–1342.
- Laufen, T., Mayer, M.P., Beisel, C., Klostermeier, D., Mogk, A., Reinstein, J., and Bukau, B. (1999). Mechanism of regulation of hsp70 chaperones by DnaJ cochaperones. *Proc. Natl. Acad. Sci. USA* **96**: 5452–5457.
- Li, G.L., Li, B., Liu, H.T., and Zhou, R.G. (2005). The responses of AtJ2 and AtJ3 gene expression to environmental stresses in *Arabidopsis*. *Zhi Wu Sheng Li Yu Fen Zi Sheng Wu Xue Xue Bao* **31**: 47–52.
- Liberek, K., Marszalek, J., Ang, D., Georgopoulos, C., and Zylicz, M. (1991). *Escherichia coli* DnaJ and GrpE heat shock proteins jointly stimulate ATPase activity of DnaK. *Proc. Natl. Acad. Sci. USA* **88**: 2874–2878.
- Lin, H., Yang, Y., Quan, R., Mendoza, I., Wu, Y., Du, W., Zhao, S., Schumaker, K.S., Pardo, J.M., and Guo, Y. (2009). Phosphorylation of SOS3-LIKE CALCIUM BINDING PROTEIN8 by SOS2 protein kinase stabilizes their protein complex and regulates salt tolerance in *Arabidopsis*. *Plant Cell* **21**: 1607–1619.
- Lino, B., Baizabal-Aguirre, V.M., and Gonzalez de la Vara, L.E. (1998). The plasma-membrane H⁺-ATPase from beet root is inhibited by a calcium-dependent phosphorylation. *Planta* **204**: 352–359.
- Lu, S., et al. (2006). The cauliflower Or gene encodes a DnaJ cysteine-rich domain-containing protein that mediates high levels of beta-carotene accumulation. *Plant Cell* **18**: 3594–3605.
- Merlot, S., Leonhardt, N., Fenzi, F., Valon, C., Costa, M., Piette, L., Vavasseur, A., Genty, B., Boivin, K., Muller, A., Giraudat, J., and Leung, J. (2007). Constitutive activation of a plasma membrane H⁺-ATPase prevents abscisic acid-mediated stomatal closure. *EMBO J.* **26**: 3216–3226.
- Mierny, J.A. (1999). Protein folding in the plant cell. *Plant Physiol.* **121**: 695–703.
- Mierny, J.A. (2001). The J-domain proteins of *Arabidopsis thaliana*: An unexpectedly large and diverse family of chaperones. *Cell Stress Chaperones* **6**: 209–218.
- Morsomme, P., and Boutry, M. (2000). The plant plasma membrane H⁺-ATPase: Structure, function and regulation. *Biochim. Biophys. Acta* **1465**: 1–16.
- Ottmann, C., Marco, S., Jaspert, N., Marcon, C., Schauer, N., Weyand, M., Vandermeeren, C., Duby, G., Boutry, M., Wittinghofer, A., Rigaud, J.L., and Oecking, C. (2007). Structure of a 14-3-3 coordinated hexamer of the plant plasma membrane H⁺-ATPase by combining X-ray crystallography and electron cryomicroscopy. *Mol. Cell* **25**: 427–440.
- Palmgren, M.G. (2001). Plant plasma membrane H⁺-ATPases: Powerhouses for nutrient uptake. *Annu. Rev. Plant Physiol. Plant Mol. Biol.* **52**: 817–845.
- Palmgren, M.G., Sommarin, M., Serrano, R., and Larsson, C. (1991). Identification of an autoinhibitory domain in the C-terminal region of the plant plasma membrane H⁺-ATPase. *J. Biol. Chem.* **266**: 20470–20475.
- Pimpl, P., Movafeghi, A., Coughlan, S., Denecke, J., Hillmer, S., and Robinson, D.G. (2000). In situ localization and in vitro induction of plant COPI-coated vesicles. *Plant Cell* **12**: 2219–2236.
- Qian, Y.Q., Patel, D., Hartl, F.U., and McColl, D.J. (1996). Nuclear

- magnetic resonance solution structure of the human Hsp40 (HDJ-1) J-domain. *J. Mol. Biol.* **260**: 224–235.
- Qiu, X.B., Guo, Y., Dietrich, M.A., Schumaker, K.S., and Zhu, J.K.** (2002). Regulation of SOS1, a plasma membrane Na⁺/H⁺ exchanger in *Arabidopsis thaliana*, by SOS2 and SOS3. *Proc. Natl. Acad. Sci. USA* **99**: 8436–8441.
- Qiu, X.B., Shao, Y.M., Miao, S., and Wang, L.** (2006). The diversity of the DnaJ/Hsp40 family, the crucial partners for Hsp70 chaperones. *Cell. Mol. Life Sci.* **63**: 2560–2570.
- Quan, R., Lin, H., Mendoza, I., Zhang, Y., Cao, W., Yang, Y., Shang, M., Chen, S., Pardo, J.M., and Guo, Y.** (2007). SCABP8/CBL10, a putative calcium sensor, interacts with the protein kinase SOS2 to protect *Arabidopsis* shoots from salt stress. *Plant Cell* **19**: 1415–1431.
- Quintero, F.J., Ohta, M., Shi, H., Zhu, J.K., and Pardo, J.M.** (2002). Reconstitution in yeast of the *Arabidopsis* SOS signaling pathway for Na⁺ homeostasis. *Proc. Natl. Acad. Sci. USA* **99**: 9061–9066.
- Richards, L.A.** (1954). Diagnosis and improvement of saline and alkali soils. In *US Salinity Lab Handbook 60*. United States Department of Agriculture. (Washington, DC: Government Printing Office).
- Rober-Kleber, N., Albrechtova, J.T., Fleig, S., Huck, N., Michalke, W., Wagner, E., Speth, V., Neuhaus, G., and Fischer-Iglesias, C.** (2003). Plasma membrane H⁺-ATPase is involved in auxin-mediated cell elongation during wheat embryo development. *Plant Physiol.* **131**: 1302–1312.
- Roelfsema, M.R.G., Staal, M., and Prins, H.B.A.** (1998). Blue light-induced apoplastic acidification of *Arabidopsis thaliana* guard cells: Inhibition by ABA is mediated through protein phosphatases. *Physiol. Plant.* **103**: 466–474.
- Schaller, A., and Oecking, C.** (1999). Modulation of plasma membrane H⁺-ATPase activity differentially activates wound and pathogen defense responses in tomato plants. *Plant Cell* **11**: 263–272.
- Scidmore, M.A., Okamura, H.H., and Rose, M.D.** (1993). Genetic interactions between KAR2 and SEC63, encoding eukaryotic homologues of DnaK and DnaJ in the endoplasmic reticulum. *Mol. Biol. Cell* **4**: 1145–1159.
- Sheen, J.** (2001). Signal transduction in maize and *Arabidopsis* mesophyll protoplasts. *Plant Physiol.* **127**: 1466–1475.
- Silver, P.A., and Way, J.C.** (1993). Eukaryotic DnaJ homologs and the specificity of Hsp70 activity. *Cell* **74**: 5–6.
- Svennelid, F., Olsson, A., Piotrowski, M., Rosenquist, M., Ottman, C., Larsson, C., Oecking, C., and Sommarin, M.** (1999). Phosphorylation of Thr-948 at the C terminus of the plasma membrane H⁺-ATPase creates a binding site for the regulatory 14-3-3 protein. *Plant Cell* **11**: 2379–2391.
- Szabo, A., Korszun, R., Hartl, F.U., and Flanagan, J.** (1996). A zinc finger-like domain of the molecular chaperone DnaJ is involved in binding to denatured protein substrates. *EMBO J.* **15**: 408–417.
- Tamura, K., Takahashi, H., Kunieda, T., Fuji, K., Shimada, T., and Hara-Nishimura, I.** (2007). *Arabidopsis* KAM2/GRV2 is required for proper endosome formation and functions in vacuolar sorting and determination of the embryo growth axis. *Plant Cell* **19**: 320–332.
- Till, B., et al.** (2003). Large-scale discovery of induced point mutations with high throughput TILLING. *Genome Res.* **13**: 524–530.
- Torii, K.U., Mitsukawa, N., Oosumi, T., Matsuura, Y., Yokoyama, R., Whittier, R.F., and Komeda, Y.** (1996). The *Arabidopsis* ERECTA gene encodes a putative receptor protein kinase with extracellular leucine-rich repeats. *Plant Cell* **8**: 735–746.
- Vera-Estrella, R., Barkla, B.J., Higgins, V.J., and Blumwald, E.** (1994). Plant defense response to fungal pathogens (activation of host-plasma membrane H⁺-ATPase by elicitor-induced enzyme dephosphorylation). *Plant Physiol.* **104**: 209–215.
- Wall, D., Zylicz, M., and Georgopoulos, C.** (1995). The conserved G/F motif of the DnaJ chaperone is necessary for the activation of the substrate binding properties of the DnaK chaperone. *J. Biol. Chem.* **270**: 2139–2144.
- Wang, W., Vinocur, B., Shoseyov, O., and Altman, A.** (2004). Role of plant heat-shock proteins and molecular chaperones in the abiotic stress response. *Trends Plant Sci.* **9**: 244–252.
- Waters, E.R., Lee, G.J., and Vierling, E.** (1996). Evolution, structure and function of the small heat shock proteins in plants. *J. Exp. Bot.* **47**: 325–338.
- Wu, J., and Seliskar, D.** (1998). Salinity adaptation of plasma membrane H⁺-ATPase in the salt marsh plant *Spartina patens*: ATP hydrolysis and enzyme kinetics. *J. Exp. Bot.* **49**: 1005–1013.
- Xing, T., Higgins, V.J., and Blumwald, E.** (1996). Regulation of plant defense response to fungal pathogens: Two types of protein kinases in the reversible phosphorylation of the host plasma membrane H⁺-ATPase. *Plant Cell* **8**: 555–564.
- Xing, T., Higgins, V.J., and Blumwald, E.** (1997). Identification of G proteins mediating fungal elicitor-induced dephosphorylation of host plasma membrane H⁺-ATPase. *J. Exp. Bot.* **48**: 229–237.
- Xu, J., Li, H.D., Chen, L.Q., Wang, Y., Liu, L.L., He, L., and Wu, W.H.** (2006). A protein kinase, interacting with two calcineurin B-like proteins, regulates K⁺ transporter AKT1 in *Arabidopsis*. *Cell* **125**: 1347–1360.
- Yan, B.C., and Yan, J.F.** (1999). Size and folding in globular proteins. *Int. J. Biol. Macromol.* **24**: 65–67.
- Yan, F., Zhu, Y., Muller, C., Zorb, C., and Schubert, S.** (2002). Adaptation of H⁺-pumping and plasma membrane H⁺-ATPase activity in proteoid roots of *white lupin* under phosphate deficiency. *Plant Physiol.* **129**: 50–63.
- Zhang, X., Wang, H., Takemiya, A., Song, C.P., Kinoshita, T., and Shimazaki, K.** (2004). Inhibition of blue light-dependent H⁺ pumping by abscisic acid through hydrogen peroxide-induced dephosphorylation of the plasma membrane H⁺-ATPase in guard cell protoplasts. *Plant Physiol.* **136**: 4150–4158.
- Zhou, R.G., and Miernyk, J.A.** (1999). Cloning and analysis of AtJ3 gene in *Arabidopsis thaliana*. *Acta Bot. Sin.* **41**: 597–602.
- Zhu, J.K., Bressan, R.A., and Hasegawa, P.M.** (1993). Isoprenylation of the plant molecular chaperone ANJ1 facilitates membrane association and function at high temperature. *Proc. Natl. Acad. Sci. USA* **90**: 8557–8561.